Elsevier Editorial System(tm) for Atmospheric Research
Manuscript Draft

Corresponding Author: Mr. enrique vieira mattos, M.D.

Corresponding Author's Institution: National Institute for Space Research

First Author: Enrique Mattos, master's degree in Atmospheric Sciences

Order of Authors: Enrique Mattos, master's degree in Atmospheric Sciences ; enrique vieira mattos, M.D.; Luiz Machado, Doctor

Abstract: This work analyzes some of the physical and microphysical properties of Mesoscale Convective Systems (MCS) and cloud-to-ground lightning. Satellite data from the GOES-10 infrared and NOAA-18 and TRMM microwave channels and lightning information from the Brazilian Lightning Detection Network (BrasilDAT) were utilized for the period from 2007 to 2009. Based on an automatic MCS detection method, 720 MCS life cycles were identified during the period and region of study, with a lightning detection efficiency of over 90%. During the diurnal cycle, the electrical activity maximum occurred close to the time of maximum convective cloud fraction and 3 hours after the maximum normalized area expansion rate. The diurnal cycles of both properties are modulated by diurnal heating and thus could be used to monitor the diurnal variability of lightning occurrence. The area growth during the initial phase of the MCS exerted a strong influence on their size-duration, and potential for electrical activity during their life cycle. The average lightning life cycle exhibited a maximum close to MCS maturation, while the maximum of the average lightning density occurred close to the initial MCS life cycle stages. The growth rate of electrical activity during the early stages can indicate the strength of convection and the possible duration of systems with lightning occurrence. The strong condensation processes and mass flux during the growth phase of the systems can provide favorable conditions for cloud electrification and lightning occurrence. A comparison of high microwave frequencies with lightning data showed a strong relationship of the vertically integrated ice content and particle size with lightning occurrence. The polarization difference in the 85 GHZ channel showed that electrical activity increases linearly with polarization reduction, associated with a high value of Pearson's correlation coefficient. This suggests that regions with more intense electrical activity are predominantly located in areas with a high concentration of larger ice particles that are preferentially oriented vertically, due to the existence of intense updrafts and the electric field. These results demonstrate the potential use of thermodynamic, dynamic and microphysical characteristics for analyzing storm severity and as additional information for monitoring of electrical activity over large regions that lack ground-based lightning sensors and for nowcasting.

Dear Editor,

This work was developed with the efforts joint of Enrique Vieira Mattos and Luiz Augusto Toledo Machado both researchers of Institute National of Space Research at Brazil. The second author this work has a great experience at cloud microphysics and convection associate the Mesoscale Convective System that was very important to development this research. The objective of the work was evaluate the relationship between Mesoscale Convective System physical and microphysical proprieties with cloud-to-ground lightning occurrence. Combined data of infrared and microwave channel of satellite with lightning occurrence from ground sensors was utilized. This newer e current study can provide potential to determine parameters of severity diagnostic and cloud-to-ground lightning nowcasting at Brazil. Moreover a great area of Brazil is hit by lightning occurrence and the few study realized in this region these characteristics make this work very importance for nowcasting products.

The Author to whom should address yours correspondence is Enrique Vieira Mattos who is named as corresponding author. The contact address is:

Mr. Enrique Vieira Mattos
Instituto Nacional de Pesquisas Espaciais (INPE)
Centro de Previsão de Tempo e Estudos Climáticos (CPTEC)
Rodovia Pres. Dutra, km 40
Cachoeira Paulista/SP - 12630-000 - Brazil
FAX: 55 - 12 – 31869291
Phone: 55 - 12 – 31869523
e-mail: enrique.mattos@cptec.inpe.br

Sincerely,
Enrique Vieira Mattos

Cloud-to-Ground Lightning and Mesoscale Convective Systems

Enrique V. Mattos*, Luiz A. T. Machado*

*Instituto Nacional de Pesquisas Espaciais-INPE,

Centro de Previsão de Tempo e Estudos Climáticos-CPTEC

Rod. Dutra, km 40, Cachoeira Paulista-SP 12630000-Brasil

Submitted to Atmospheric Research

May – 2010

Corresponding Author Addresses:

Instituto Nacional de Pesquisas Espaciais (INPE)
Centro de Previsão de Tempo e Estudos Climáticos (CPTEC)
Rodovia Pres. Dutra, km 40
Cachoeira Paulista/SP - 12630-000
Brazil
FAX: 55 - 12 – 31869291
Phone: 55 - 12 – 31869523
e-mail: enrique.mattos@cptec.inpe.br

Abstract

This work analyzes some of the physical and microphysical properties of Mesoscale Convective Systems (MCS) and cloud-to-ground lightning. Satellite data from the GOES-10 infrared and NOAA-18 and TRMM microwave channels and lightning information from the Brazilian Lightning Detection Network (BrasilDAT) were utilized for the period from 2007 to 2009. Based on an automatic MCS detection method, 720 MCS life cycles were identified during the period and region of study, with a lightning detection efficiency of over 90%. During the diurnal cycle, the electrical activity maximum occurred close to the time of maximum convective cloud fraction and 3 hours after the maximum normalized area expansion rate. The diurnal cycles of both properties are modulated by diurnal heating and thus could be used to monitor the diurnal variability of lightning occurrence. The area growth during the initial phase of the MCS exerted a strong influence on their size-duration, and potential for electrical activity during their life cycle. The average lightning life cycle exhibited a maximum close to MCS maturation, while the maximum of the average lightning density occurred close to the initial MCS life cycle stages. The growth rate of electrical activity during the early stages can indicate the strength of convection and the possible duration of systems with lightning occurrence. The strong condensation processes and mass flux during the growth phase of the systems can provide favorable conditions for cloud electrification and lightning occurrence. A comparison of high microwave frequencies with lightning data showed a strong relationship of the vertically integrated ice content and particle size with lightning occurrence. The polarization difference in the 85 GHZ channel showed that electrical activity increases linearly with polarization reduction, associated with a high value of Pearson's correlation coefficient. This suggests that regions with more intense electrical activity are predominantly located in areas with a high concentration of larger ice particles that are preferentially oriented vertically, due to the existence of intense updrafts and the electric field. These results demonstrate the potential use of thermodynamic, dynamic and microphysical characteristics for analyzing storm severity and as additional information for monitoring of electrical activity over large regions that lack ground-based lightning sensors and for nowcasting.

Keywords: Lightning, Mesoscale Convective System, Cloud Microphysics, Nowcasting

1. Introduction

The importance of the dynamic, thermodynamic and microphysical parameters of Mesoscale Convective Systems (MCS) in producing lightning activity has been the subject of various studies. MCS have been shown to be efficient producers of much of the precipitation in the tropics and in the summer in mid-latitudes, and are typically associated with severe weather conditions (lightning, intense precipitation, hail, strong winds, and flooding) in various regions of the world (Maddox, 1980; Goodman et al., 1986, Velasco and Fritsch, 1987; Machado et al., 2004). However, few studies exist which relate cloud-to-ground lightning (henceforth referred to as CG lightning) with cloud properties estimated from orbital sensors. Advances in understanding of the impacts of MCS morphological and radiative characteristics on the intensification of convection and electrical activity, and thus the influence of CG lightning on weather and climate, would contribute to the nowcasting of extreme weather events. In this way, investigations of the physical and microphysical processes involved in MCS convective and electrical activity could help determine severity parameters and improve forecasts in tropical regions.

The factors responsible for the formation and development of these thunderstorms are not yet completely understood. However, it has been accepted that the collision of ice particles (ice crystals and hail) and super-cooled water is an important process for cloud electrification (Reynolds, 1957; Saunders, 1993). The non-inductive collision process has suggested that charge centers of opposite polarity formed inside cloud can it, produce an intense electric field (hundreds of KV/m) capable of breaking the dielectric rigidity of the air and driving the formation of electric discharges (Baker and Dash, 1989; Keith and Saunders, 1990; Tsenova et al., 2009). Thus, the physical and microphysical properties and their simultaneous interactions have revealed important aspects of thunderstorm electrical activity.

The thermal infrared window channels (IR, 10.2-11.2 μm) of geostationary satellites have revealed prominent characteristics of the tops and organization of clouds associated with severe convection. In one of the pioneering works, Goodman et al. (1986) noted that half of the Mesoscale Convective Complexes (MCC) observed over Oklahoma caused damages associated with lightning, which is the most frequent between the development and mature stages of the MCC. On the other hand, Parker et al. (2001) verified that for three distinct middle-latitude MCS, the maximum CG lightning, both positive and negative, occurred before the maximum system size was reached. Using an automatic cloud tracking and identification method, Tadesse and Anagnostou (2009) showed that the majority of systems with lightning have duration of

an hour longer than the others, in addition to exhibiting more intense electrical activity close to the maturation stage. Over the southern region of Brazil, Lima and Gomes (2009) analyzed three MCS using a semi-automatic method and verified that the CG lightning maximum was close to maturation and associated with intense convection. The work of Machado and Laurent (2004) suggested that this life cycle phase corresponds to the moment of maximum high-level divergence and a decrease in the condensation rate, that is, the moment in which the maximum convective cloud cover is achieved.

Clouds with low top temperatures have been predominantly observed in regions of more intense electrical activity (Vonnegut, 1953; Williams, 1985; Goodman and Macgorman, 1986; Ushio et al., 2001, Dotzek et al., 2005, Scofield et al, 2005; Altaratz et al., 2010). Williams (1985) observed that the lightning rate is a function of the fifth power of the cloud height, while Ushio et al. (2001) verified that the relationship has approximately exponential global behavior for winter/summer in the extratropics and ocean/continent in the tropics. Recently, Altaratz et al. (2010) observed that during the dry season in the Amazon region, the quantity of strokes increased as a function of the decrease in cloud top pressure (linear relationship) and increase in the convective cloud fraction (exponential relationship). For cloud top temperature, Goodman and Macgorman (1986) found an increased occurrence of lightning for temperatures below approximately 200 K, while Dotzek et al. (2005) observed a threshold of 203 K below overshooting tops with a V shape. Machado et al. (2009) showed that penetrating clouds are associated with electrical discharges and that there is an increased probability of CG electrical discharges with an increase in the difference in brightness temperature between the infrared window channel and water vapor. Despite the different limits found over various regions, a common characteristic is the existence of a high correspondence between the average cloud top temperature of the MCS in the IR and the occurrence of lightning.

Many studies using models of cloud electrification have shown the existence of an interdependent relationship of electrical activity with the size, concentration, ice particle phase (Keith and Saunders, 1990; Mitzeva and Saunders, 1990; Baker et al., 1995; Miller et al., 2001; Tsenova et al., 2009) and availability and distribution of super-cooled liquid water drops (Saunders et al., 1991) and the impact velocity of the particles (Mitzeva and Saunders, 1990; Brooks et al., 1997). However, a smaller number of studies have characterized this relation using microwave satellite estimates. Keith and Saunders (1990) and Miller et al. (2001) used numerical storm modeling and observational data to show that the amount of charge transferred in the collisions

between ice particles can depend nonlinearly on size. In addition, some studies have shown that an increased occurrence of lightning tends to be associated with an increase in the storm ice content (Baker et al., 1995; Blyth et al., 2001). The work of Petersen et al. (2005) has suggested that on the global scale the relation between ice content and lightning is approximately linear, and invariable over continental, oceanic, and coastal regions. On the other hand, the results of Spencer et al. (1989) and Prigent et al. (2001) have suggested that the orientation (vertical or horizontal) of ice particles can be investigated using the differences in T_B at 85 GH (T_{BV}-T_{BH}). They verified that more negative (positive) values indicate regions with more intense (less intense) storm convection. Prigent et al. (2005) observed an increase in the probability of lightning from 15% to 45% associated with a decrease of T_{BV}-T_{BH} from 7 K to -5 K, for observations from the TRMM Microwave Imager (TMI) sensor and lightning observations from Lightning Imaging Sensor (LIS, Intra-cloud + Cloud-to-ground lightning) from Tropical Rainfall Measuring Mission (TRMM).

The objective of this work is to investigate the physical relationship among MCS dynamic, thermodynamic and microphysical parameters and the occurrence of CG lightning, through the utilization of infrared channel and passive microwave information originating from satellites together with lightning information obtained from ground-based sensors. In this way, the potential of these parameters to be utilized as indicators of severity and in the prediction of electrical activity will be evaluated.

Section 2 describes the CG lightning and satellite data used and the methodology employed in this work. Section 3 presents the diurnal cycle results and the relationships of the life cycle and physical and microphysical properties with CG lightning electrical activity. Finally, the conclusion is presented in Section 4.

2. Data and Methodology

2.1. The BrasilDAT Network

The CG lightning data used in this study were provided by the Brazilian Atmospheric Electrical Discharge Detection Network (BrasilDAT). BrasilDAT operates at Low Frequency (LF) and Very Low Frequency (VLF), and is composed of 46 sensors covering the South and Southeast regions and part of the North of Brazil. Sensors using the Lightning Position and Tracking System (LPATS) and Improved Accuracy Using Combined Technology (IMPACT) technologies are employed. The combination of the distribution geometry with the technology utilized by the sensors results in an average

precision of 500 m in locating CG lightning sources and a detection efficiency of 90% in some parts of the country (Pinto et al., 2007). The BrasilDAT data employed in the present work consist of the location, date and time of CG lightning occurrences for the period of May 2007 to August 2009 over an area centered in the state of São Paulo, demarcated by the coordinates 53ºW to 44ºW and 26ºS to 19ºS. This area was chosen as the standard for the study, because it is concentrated in the region of Brazil with the best and most homogeneous lightning coverage, resulting in a detection efficiency of over 90%. Figure 1 shows the study area, indicated by the rectangle in bold, and the sensors located in this region, as well as the detection efficiency contour lines.

2.2. Infrared Satellite Data

Brightness temperature data from the IR (10,2-11.2 μm) channel images from the GOES-10 satellite, received by CPTEC/INPE, were employed to determine the physical properties of the MCS. The images were obtained in satellite projection and were reprojected to a rectangular projection covering all of South America for the period of May 2007 to August 2009, with a temporal resolution of 15 minutes and a spatial resolution of 4 km (sub-satellite point). The obtained images were assimilated by the Forecast and Tracking of Active Convective Cells (ForTraCC) algorithm in order to track the MCS life cycle for the above mentioned period.

ForTraCC is an algorithm presented by Vila et al. (2008) that determines the trajectories and life cycle of these systems through successive IR images, based on the morphological characteristics and the superposition of areas between the images. A minimum size of 90 pixels and a threshold of 235 K and 210 K were defined in order to detect the MCS and Convective Cells (CC), respectively. This procedure produces a time series of physical properties (morphological and radiative characteristics) of the MCS through their life cycle, such as: location, size, normalized area expansion rate, average and minimum brightness temperature, convective fraction, eccentricity, inclination angle, and other parameters (more details in Machado et al., 1998). Only MCS were selected that passed over the São Paulo state at some point in their life cycle, and 16,520 such systems were identified during the study period. For each moment in the system life cycle, occurrences of lightning were counted from 7.5 minutes before until 7.5 minutes after the image time. Statistical analyses were conducted with the aim of understanding the diurnal cycle and the relationships between the physical properties and CG lightning. The dispersion analyses considered Pearson's correlation coefficients and p-values with a significance level of 0.01.

The MCS life cycle study was conducted considering only systems that: (1) initiated spontaneously (that is, that did not originate as the result of a MCS split) and ended by dissipation (that is, did not end by merging with other systems) in the interior of the study area; and (2) had few missing images (less than half the total lifetime). The first limitation assures that the initial growth of the system was due to its internal dynamics and that its lifetime was representative of the entire lifetime, as discussed by Machado and Laurent (2004). In addition, it assures that the systems were always located over an area with lightning detection efficiency that was constant and over 90%. Thus, 420 systems were identified with lightning (henceforth denominated Thunderstorms) and 300 without lightning (henceforth denominated Storms). It should be remembered that this work only considers cloud-to-ground discharges, while there can be intra-cloud (IN) and cloud-to-cloud (CC) discharges that are not considered. Thus, the specific denomination of Storm and Thunderstorm in this study is based only on the CG lightning condition.

2.3. Passive Microwave Satellite Data

The estimates of the effective ice particle diameter (D_e) and the Ice Water Path (IWP) were made using an inference algorithm similar to that presented by Zhao and Weng (2001). The processing of this model was accomplished using the T_B from the 23 GHz and 31 GHz channels of the Advanced Microwave Sounder Unit-A2 (AMSU-A2) sensor and the 89 GHz, 157 GHz and 183.3 ± 1 GHz channels of the Microwave Humidity Sounder (MHS) sensor of the NOAA-18 satellite. These data were received by CPTEC/INPE and cover the period of January 2007 to September 2009. The parameterizations for estimating the values of D_e and IWP are determined by combining empirical and statistical methods similar to those presented by Zhao and Weng (2001), and can be expressed as

$$D_e = a_0 + a_1 r + a_2 r^2 + a_3 r^3 \qquad \text{and} \qquad (1)$$

$$IWP = \mu D_e \rho_i \left(\Omega_{89or157} / \Omega_N \right), \qquad (2)$$

where a_0, a_1, a_2 and a_3 are the regression coefficients that depends on the volumetric density of the ice particles (ρ_i, in kg/m^3) and the size distribution of the particles and r is the scattering ratio between the 89 GHz and 157 GHz channels. The parameters associated with the IWP calculation are: μ, ρ_i, $\Omega_{89or157}$ and Ω_N, which are the cosine of the zenith angle, the volumetric density of the ice particles, the scattering coefficient

in both channels and the normalized scattering coefficient. Thus, the empirical relation (Eq. 2.1) between D_e and r is determined based on simulated data from a radiative transfer model (see Weng, 1992 and Zhao and Weng, 2001). Therefore, for the study region, a volumetric ice density of 920 kg/m^3 was used, and the regression coefficient values utilized are shown in Table 2.1. The 89 GHz channel is insensitive to signal scattering originating from small particles, thus the ratio between the scattering coefficients at 89 GHz and 157 GHz expresses the scattering by a greater range of particles. This ratio is expressed as

$$r = \frac{\Omega_{89}}{\Omega_{157}}, \tag{3}$$

where Ω_{89} and Ω_{157} are the scattering coefficients in the 89 GHz and 157 GHz channels, respectively. Based on a two stream approximation similar to that presented by Weng and Grodoy (2000), the scattering coefficient for both channels (Ω_{89} and Ω_{157}) is determined using the difference between the temperature of the cloud base T_b and top T_t, normalized by the value of the cloud top temperature, expressed as

$$\Omega_{89or157} = \frac{T_{b(89or157)} - T_{t(89or157)}}{T_{t(89or157)}}. \tag{4}$$

The cloud top brightness temperatures in both channels ($T_{t_{89}}$ and $T_{t_{157}}$) are estimated by the NOAA-18 satellite and corrected considering the local zenith angle. On the other hand, cloud base temperature ($T_{b_{89}}$ and $T_{b_{157}}$) for the continent is estimated using the empirical relationship between the low frequencies of the AMSU-A2 sensor (23 and 31 GHz) and the high frequencies of the MHS sensor, as presented by Zhao and Weng (2001). This expression is defined as

$$T_{b_{89}} = 17.88 + 1.61 T_{t23} - 0.67 T_{t31} \quad \text{and} \tag{5}$$

$$T_{b157} = 33.78 + 1.69 T_{t23} - 0.80 T_{t31}. \tag{6}$$

In this way, the empirical relation between D_e and r is used to determine the size of the ice particles considering only values of the scattering coefficient (r) less than 0.8. Thus, the condition for a detectable cloud considers only temperatures at 183.3 GHz of less

than 265 K. For D_e less than (greater than) 1 mm the Ω_{157} (Ω_{89}) is used in Eq. 2.2 and the parameters μ (determined using the local zenith angle), D_e, ρ_i (920 kg/m^3) are also used, while Ω_N is determined by

$$\Omega_N = \exp\left[b_0 + b_1 \ln(De) + b_2 \left(\ln(De) \right)^2 \right], \tag{7}$$

where b_0, b_1, b_2 and b_3 are the regression coefficients for the values of D_e above and below 1 mm. The values of these coefficients used for both classes of D_e are shown in Table 1.

The effects of boundary pixel deformation were eliminated at the threshold of the viewing angle (Local Zenith Angle) between $\pm 25°$ (Bernnartz, 2000; Stubenrauch et al., 2004), considering that at the sub-satellite point (footprint), the spatial resolution is 20 km by 16 km. For each pixel, a search was made for CG lightning occurrences from 7.5 minutes before until 7.5 minutes after the time of the scanned line. Statistical analyses of dispersion and standard deviation associating D_e and IWP with CG lightning were conducted, evaluated with Pearson's correlation coefficients and p-values with a significance level of 0.01.

The T_B from the 85 GHz channel with vertical (T_{BV}) and horizontal (T_{BH}) polarization from the TMI sensor onboard the TRMM satellite were used to estimate the orientation of the ice particles. As discussed by some authors (Prigent et al., 2001; Prigent et al., 2005), the temperature difference (T_{BV}-T_{BH}) at 85 GHz can indicate the region and preferential orientation type (vertical or horizontal) of the ice particles associated with electrical activity. For the region and period of study cited above, only pixels with a Polarization Corrected Temperature (PCT) less than 250 K were selected in order to avoid signals not originating from convective clouds (similar to Spencer et al., 1989; Mohr et al., 1996; Mohr and Zíper, 1996; Cecil et al., 2002; Biscaro and Morales, 2008). Thus, for each pixel the difference T_{BV}-T_{BH} was determined and the occurrences of lightning were counted from 7.5 minutes before until 7.5 after the time of the scanned line in an elliptical region of 7 km by 5 km centered at the pixel position. Statistical analyses similar to those discussed above for other parameters were also applied to the relationships of T_{BV}-T_{BH} with the occurrence of CG lightning.

3. Results

3.1. The diurnal cycle of the MCS area expansion and convective fraction and CG lightning

The diurnal cycles of the physical properties were evaluated only for the moments of the life cycle when the systems were passing over the region of study, considering only the cases without Split (division of systems) and Merge (fusion of systems). The 16,520 MCS identified over the area and during the analyzed period (2007-2009) were associated with 951,359 occurrences of CG lightning. Figure 2 shows the average variation over the diurnal cycle of the normalized expansion rate ($10^{-6}*s^{-1}$), convective fraction and the total number and the density of lightning (# CG lightning/$km^2*15min$) associated with the analyzed MCS. The normalized area expansion rate is the variation of the system size between two consecutive images (during this study the time interval was 15 minutes) normalized by the average area, while the convective fraction represents the ratio between the number of pixels with $T_B < 210$ K and $T_B < 235$ K, which corresponds to the total MCS area. These parameters exhibit a coherent and organized in phase behavior, achieving maximum intensity during the afternoon and beginning of the night. The maximum electrical activity occurs at the end of the afternoon, associated with the daytime convection forced by solar heating. The same result was also observed in the United States (Orville et al., 2000), Austria (Schulz et al., 2005), Europe (Manoochehrnia et al., 2007) and Brazil (Pinto et al., 2003). An intense increase in the area of the convective systems is noted after 12 GMT, attaining a maximum 3 hours before the moment of the maximum record of total lightning count. After this moment the growth rate of the systems decreases drastically. Figure 2 shows that the greatest density of lightning accompanies the abrupt increase in area expansion between 14 and 16 UTC. This is the moment of the formation and development of the systems prior to the mature phase, in which the convective processes are very intense. Since the area expansion is associated with the mass flux in the inside the cloud (Machado and Laurent, 2004), it is expected to be one of the moments of maximum electrification of the convective system. However, it is noted that the maximum total number of observed lightning occurs later, after 16 UTC, when the system attains the largest size and convective fraction. It is noted that the existence of the largest convective fractions during the night, associated with a large number of electrical discharges, is probably due to systems of long duration that consequently attain large convective areas. These results indicate that the density of electrical activity is highest

at the moment when the clouds are growing and have the most intense convective cells, and that the largest number of electrical discharges occurs when the system is close to maturation, attaining the largest convective area.

3.2. Relationship of Convective System area and temperature with CG lightning

The analysis of MCS physical properties evaluated the interdependence of the cloud horizontal dimension (dynamical aspect) and top height (thermodynamic aspect) with CG lightning occurrence. Figure 3 presents the average variation in the number of CG lightning (# CG lightning by MCS in 15 minutes intervals) as a function of the effective radius (km) of the systems and the associated standard deviation. The effective radius corresponds to the radius of a circle whose size is equal to the area of the MCS. A rapid area growth is associated with a strong increase in electrical activity (as noted in the high correlation coefficient R = 0.96, pv = 9.63×10^{-11}). Thus, an increase of approximately 22 % in the electrical activity is preceded by a 50 % increase in the area of the systems. However, this relationship is valid on average and only considers the factor of the cloud cluster area, because as is evidenced by the literature, the electrical activity is dependent on a complex combination of physical and microphysical characteristics. It is interesting to note that a recent completely independent study (Altaratz et al., 2010) found a more intense production of lightning associated with the largest cloud cover over the Amazon region. In agreement, these large areas are associated with strong high level wind divergence, which is due in part to intense updrafts (mass flux) in deep convective clouds capable of sustain and intensify the mutual interaction of ice particles involved in the electrification process. These dynamical characteristics of mesoscale cloud organization have also been observed in studies such as Machado et al. (2004) for the Amazon region and Tadesse and Anagnostou (2009) for the United States.

Figure 4 shows the average relationship between the number of CG lightning (# CG lightning by MCS in 15 minutes intervals) and the minimum cloud top temperature (K). In this case the temperature corresponds to the average of the nine coldest pixels belonging to the convective towers embedded in the inside of the MCS. In this figure, it can be noted that the clouds with the highest tops (lowest brightness temperature) are strongly correlated (R = 0.84, pv = 1.24×10^{6}) with the regions with the most electrical activity. Some of the qualitative similarities of these results have been observed in various studies. In agreement, the results of Williams (1985) and Ushio et al. (2001) have suggested a nonlinear relationship between lightning and cloud height, while in

support of these observations, Goodman and Macgorman (1986) and Scofield et al. (2005) verified intense electrical activity for the lowest cloud top temperatures. Although the temperature thresholds were found to be different in diverse regions (which could be associated with local meteorological conditions, tropopause height or the conditions for the definition of the systems), in general an intensification of the electrification processes by the deepest clouds has been observed.

The results indicate that there is a combined effect of regions of intense deep clouds extending to the lowest temperatures and strongest vertical velocities. These aspects show the influence of the existence of large areas with mixed phase hydrometeors that would lead to the formation of an intense charge center and trigger lightning. Another important aspect is that only temperatures below 210 K are characterized by a significant increase in the average electrical activity growth rate. For values above this threshold, the relationship has low significance and is approximately linear. This is an indication that this region could be associated with areas with the most intense cold tops, which could possibly produce thermodynamic conditions more conducive to a more intensive production of ice particles (Wallace and Hobbs, 1977). The largest standard deviations for the lowest temperatures are associated with the few events in this class range.

3.3. Convective System Life Cycle Characteristics

For the period (May 2007-August 2009) and region analyzed, and considering the limitations previously discussed, from a total of 16,520 MCS life cycles, only 720 systems remained that satisfied the requirements of passing over the target area and having few missing images and that did not initiate and dissipate as Merge and Split. Among the systems tracked and identified by the ForTraCC algorithm, a total of 420 presented at least one CG lightning during their life cycle, while in 300 systems no occurrences of CG lightning were detected. The differences between Storm and Thunderstorm are, however, initially analyzed in terms of the total life cycle duration. Figures 5a and 5b show the distribution of accumulated and relative frequency (in percentage) of total duration for systems without and with CG lightning, respectively. For both groups of systems, there is a predominance of those with shorter duration, which was to be expected since there is an almost linear relationship between size and duration, with the smaller ones (or those with shorter duration) much more numerous than the larger ones (or those with longer duration). However, the characteristic that is highlighted in these results is that the duration of the Thunderstorms (at the 90 % level),

on average, is one hour longer in relation to the Storms. It is noted that 26% of the population of Storms have duration of less than 1.5 hours, while for the Thunderstorms this population is only 16%. The longer duration of the Thunderstorms in relation to the Storms suggests the existence of more vigorous convection during the initial stages, sustaining the systems for a longer period. This indicates that the dynamic forcing during the initiation of the systems is important for the intensification of convection and charging processes in the cloud interior.

The MCS life cycle can be classified through the evolution of the area as initiation (first time detected), mature (maximum area) and dissipation (last time detected) stage. The average variation of the area (effective radius in km) during the life cycle of the Storms and Thunderstorms with total duration of 1-5 hours are shown in Figures 5c and 5d, respectively. The area increases rapidly during the first stages of life, growing at a slower rate until reaching maturation close to the half life of the systems, followed by a strong decay of area during the dissipation stage. Another commonly observed aspect is that the systems of longer duration simultaneously present larger areas throughout the life cycle and a more intense initial area expansion. The works of Machado and Laurent (2004) and Tadesse and Anagnostou (2009) also suggested that the growth rate during the initial stage is a parameter indicative of the degree of convection severity. On the other hand, the Thunderstorms present a larger initial expansion of the area and the largest areas during the lifetime evolution. For an average lifetime of 4 hours, the systems with lightning present an average initial expansion three times larger in relation to the Storms with the same duration and two times less intense than those with 5 hours of duration from the same group of Thunderstorms. This analysis suggests that the initial stage of the Thunderstorms is composed of the more intense updrafts capable of creating clouds with higher tops and a larger liquid water content, which can intensify the convective activity and consequently the lightning occurrence.

Figure 6a presents the average values of the evolution throughout the life cycle of the relative frequency of the total CG electrical discharges (percentage of total CG lightning observed during the MCS life cycle) and the relative MCS size of MCS ((size_MCS(t)/size_MCS(mature stage))*100, where size_MCS(t) is the radius of the MCS at the time t) for five life cycle stages: initiation - the first time that the system was detected (stage 1); the intermediate stage between initiation and maturation (stage 2); maturation - maximum size (stage 3); intermediate between maturation and dissipation (stage 4) and dissipation - the last time that the system was detected (stage 5). The period of most intense electrical activity is found between initiation and maturation (50 % of the total CG lightning occur between stages 1 and 2 and 80 %

before maturation), while a less pronounced occurrence of lightning is observed after this stage (less than 20 % of the lightning occurred during the last two stages). It is noted that a strong increase in the number of lightning and MCS area occurs during the first two life cycle stages. The maximum lightning occurrence is observed in stages 2 and 3, while 33 % of the occurrences are observed solely in the mature phase. A rapid decrease in electrical activity is observed in phases 4 and 5, probably due to the weakening of convective processes in the dissipation phases. Parker et al. (2001) found a maximum of both positive and negative CG lightning close to maturation, and the same has been observed for analyses of total lightning (Goodman and Macgorman, 1986; Tadesse and Anagnostou, 2009). A similar behavior (Figure 6b) of the evolution of the average number of the total CG lightning by MCS inside 15 min intervals is observed for discrete MCS life time from 1 to 4 hours. This result suggests that to the degree to which the MCS present longer life cycle duration, the later the maximum electrical activity occurs, between the initiation and maturation stages. Based on these results, the most intense electrical activity during the initial stages is associated with a high condensation rate combined with intense mass flux and growth of MCS area. Indeed, it is during this stage that the systems minimum brightness temperatures and maximum convective cells area merged inside the MCS are observed (Machado et al., 1998). The formation and interaction of ice particles is enabled during these stages, leading to a more intense electrification process.

Complementing the results found above, the maximum relative frequency of lightning density is found during the initiation (Figure 6c). The same occurs for discrete life time values of CG lightning density (number of CG lightning by km^2 in 15 minutes intervals) as shown in Figure 6d. Consistently, it can also be noted that the shorter the MCS life time, the more quickly the electrical activity maximum is obtained. The high discharge density in the first stages indicates that the convection process during this stage is more localized in the predominant convective clouds in this life cycle phase. As the MCS evolves, it becomes composed of a large quantity of cirrus and stratiform clouds, which are much less efficient in producing electrical discharges. During dissipation, the systems are smaller; however, the convection is much less intense, naturally leading to a lower electrical activity.

3.4. Microphysical Proprieties

As previously discussed, the analysis of the D_e and IWP parameters considered only pixels with local zenith angle between $\pm 25°$ and over the studied region and during the

period (January 2007 to September 2009) of study. This resulted in the identification of approximately 6,027 events (number of NOAA pixels) associated with a total of 35,811 CG lightning occurrences. Figure 7 shows the average behavior of the lightning occurrences (# CG lightning/pixel*15 min) by pixels in 15 minutes intervals as a function of the effective ice particle diameter (D_e, in mm). In general, an average increase in the occurrence of CG lightning is associated with an increment in the size of the ice particles, as shown by the high determination index (R = 0.86, pv = 2.11×10^{-6}). However, a relationship between these two variables is only noted for D_e greater than 1 mm. Consistent with these results, Zhao and Weng (2001) found the largest ice particles (diameter of 0.9-1.2 mm) present in the most intense convective regions of mid-latitude storms, while Keith and Saunders (1990) verified a nonlinear dependence on the quantity of charge transferred between particles of this size. This suggests that ice particles smaller than 1 mm do not have a sufficient contact area for the collisions in the cloud interior to lead to an efficient charge transfer. The decrease in the occurrence of lightning above 1.6 mm ice particle diameter and high standard deviation values can be attributed to large ice particles not associated with active convective clouds, yet the small number of observed events in these classes does not permit the extraction of precise information.

The average lightning electrical activity (# CG lightning/pixel*15 min) varies in an approximately linear form (R = 0.96, pv = 3.49×10^{-12}) with the IWP as showed at Figure 8. One increase over 0.5 kg.m^{-2} on ice content represent an average increase of six CG lightning. Similar results have been observed correlating total lightning data (IN+CG) originating from LIS and TMI (Baker et al., 1995; Blyth et al., 2001). These results indicate that the larger availability of ice particles in the cloud interior could intensify the collision rate, leading to a larger quantity of electrified particles and intensifying the electrification process. Nevertheless, it is noted that the IWP can play an important role in other forms of electric charge transfer during the collisions. On the other hand, a point to be observed is that strong electrical activity occurs for a large range of the IWP values, while for the D_e analyses this only occurs above a threshold. This suggests that the ice content is important during the occurrence of the lower electrical activity rates, while for the largest convection intensities D_e has a slightly more effective role.

The analysis of the interdependence of the electrical activity with relation to the polarization of the ice particles identified 13,207 events (number of TRMM-TMI pixels) associated with 37,302 CG lightning occurrences. Thunderstorms possess important peculiarities in relation to the preferential ice particle orientation in their interior, which can be revealed by the difference in polarization in the 85 GHz channel

(T_{BV}-T_{BH}). The decrease in the difference in polarization (more negative differences, that is, those associated with regions with particles preferentially oriented in the vertical) is associated with a large increase in the number of lightning events (Figure 9). Indeed, that this characteristic is also revealed by the high determination coefficient (R = 0.93, pv = 1.18×10^{-7}) demonstrates that intense convective centers are capable of attenuating the vertically polarized radiation in a more efficient manner. Previous studies have also observed this characteristic for total lightning (CG plus IN) (Prigent et al., 2005) as well as for only CG lightning (Spencer et al., 1989). The explanation consists of the existence of strong updrafts and an intense vertical electric field capable of aligning them preferentially in the vertical. This orientation is capable of more effectively attenuating the polarized signal vertically as opposed to that which propagates in the horizontal direction. Thus, these results indicate that a combination of information at 85 GHz (vertical and horizontal polarization) can provide a reasonable approximation of location and preferential symmetry axis orientation of these particles, and consequently identify regions more suitable for triggering the occurrence of lightning.

4. Conclusion

This study combined information originating from infrared and microwave channels and occurrences of CG lightning in order to evaluate the relationship among physical and microphysical properties and electrical activity in mesoscale convective systems. An automatic MCS tracking method was applied over an area with a constant lightning detection efficiency above 90 % from 2007-2009. The diurnal cycle analysis showed an electrical activity maximum close to the time of maximum convective fraction and 3 hours after the maximum rate of area expansion. It can also be concluded that the area expansion can be used as an indicator parameter of the time of maximum lightning density during the diurnal cycle. The maximum lightning density occurs a few hours before the maximum total lightning occurrences, since the maximum is also associated with the development of a larger convective area. Among the physical properties evaluated, the size and minimum brightness temperature of the MCS showed the strongest correlations with the convection intensity and the lightning frequency. This suggests that the updraft intensities and the heights of the convective towers embedded in these systems are relevant parameters for the identification of the storm severity and immediate weather prediction.

The initial area expansion was shown to be a strong parameter for defining the stage of development and potential of the systems to produce electrical activity. The Thunderstorms showed a well defined life cycle in relation to the Storms, with a longer life time and larger area. The maximum lightning frequency occurs during the growth phase close to maturation, while the average lightning density attains the maximum during the first life cycle stages. A lower electrical activity intensity was observed after achieving maturation. The physical explanation for these results is based on the combination of the intense condensation rate and mass flux during the development period of the systems, enabling an intensification of the convective cloud electrification processes and the later increase in MCS convective area but also with others cloud types some of them unable to develop electrical activity.

The ice size and content showed a strong positive correlation with lightning, as was also found in previous studies over other regions. These results demonstrated that a high availability of the largest ice particles is a relevant microphysical characteristic for the formation of intense charge centers and the initiation of electrical activity. A significant increase in electrical activity was observed only for ice particles larger than 1 mm. The polarization difference at 85GHz showed potential as a technique for identifying regions of more intense convection associated with ice particles oriented preferentially in the vertical.

The analyses demonstrated that aspects such as MCS size and minimum brightness temperature combined with information about cloud microphysics could be useful parameters for the immediate prediction of electrical activity and diagnosis of severity. Also, the assimilation of microphysical parameters in synergy with lightning occurrence in medium-term prediction models could also be relevant additional information.

The physical and microphysical processes involved in cloud electrification and the occurrence of lightning is shown to be extremely complex and dependent on numerous variables. However, a set of cloud physical parameters showed to provide new tools for monitoring and forecasting electrical discharge in MCS and an important background for the understanding of the cloud processes.

Acknowledgments

References

Altaratz, O., Koren, I., Yair, Y., Price, C., 2010. Lightning response to smoke from Amazonian fires. Geophys. Res. Lett. 37, L07801. doi:10.1029/2010GL042679.

Baker, M. B., Christian, H. J., Latham, J., 1995. A computational study of the relationships linking lightning frequency and other thundercloud parameters. Q. J. R. Meteorolog. Soc. 121, 1525-1548.

Baker, M. B., Dash, J. G., 1989. Charge-transfer in thunderstorms and the surface melting of ice. J. Cryst. Growth. 97, 770-776.

Bennartz, R., 2000. Optimal convolution of AMSU-B to AMSU-B. J. Atmos. Oceanic Technol. 17, 1215-1225.

Biscaro, T. S., Morales, Carlos A., 2008. Continental passive microwave-based rainfall estimation algorithm: application to the Amazon Basin. J. Appl. Meteorol. 47, p.1962.

Blyth, B. M., Christian, H. J., Driscoll, K., Gadian, B. M., Latham, J., 2001. Determination of ice precipitation rates and thunderstorm anvil ice contents from satellite observations of lightning. Atmos. Res. 59-60, 217-229.

Brooks, I. M., Saunders, C. P. R., Mitzeva, R. P., Peck, S. L., 1997. The effect on thunderstorm charging of the rate of rime accretion by graupel. Atmos. Res. 43, 277-295.

Cecil, D. J., Zipser, E. J., Nesbitt, S. W., 2002. Reflectivity, ice scattering, and lightning characteristics of hurricane eyewalls and rainbands. part I: quantitative description. Mon. Weather Rev. 130, 769-784.

Dotzek, N., Rabin, R. M., Carey, L. D., MacGorman, D. R., McCormick, T. L., Demetriades, N. W., Murphy, M. J., Holle, R. L., 2005. Lightning activity related to satellite and radar observations of a mesoscale convective system over Texas on 7–8 April 2002. Atmos. Res. 76, 127-166.

Goodman, S. J., Macgorman, D. R., 1986. Cloud to ground lightning activity in Mesoscale Complexes Convective. Mon. Weather Rev. 114, 2320-2328.

Keith, W. D., Saunders, C. P. R., 1990. Further laboratory studies of the charging of graupel during ice crystal interactions. Atmos. Res. 25, 445-464.

Lima, K. C., Gomes, R. G., 2009. Detecção de descargas elétricas atmosféricas em Sistemas Convectivos com dados do Simepar. Braz. J. Geophys. 27(1), 5-16.

Machado, L. B. T., Laurent, H., 2004. The Convective System area expansion over Amazonia and its relationships with Convective System life duration and high-level wind divergence. Mon. Weather Rev. 132, 714-725.

Machado, L. B. T., Lima, W. F. S., Pinto Jr, O., Morales, C. B., 2009. Relationship between cloud-ground discharge and penetrative clouds: a multi-channel satellite application. Atmos. Res. doi:10.1016/j.atmosres.2008.10.003.

Machado, L. B. T., Rossow, W. B., Guedes, R. L., Walker, B. W., 1998. Life cycle variations of Mesoscale Convective Systems over the Americas. Mon. Weather Rev. 126, 1630-1653.

Maddox, R. B., 1980. Mesoscale Convective Complexes. Bull. Amer. Meteor. Soc. 61, 1374-1387.

Manoochehrnia, P., Rachidi, F., Rubinstein, M., Schulz, W., 2007. Lightning Statistics In Switzerland. In: International Symposium On Lightning Protection, 9., 2007, Foz do Iguaçu. Proceedings...7 p., Foz do Iguaçu, Brazil: EPFL, 2007.

Miller, K., Gadian, B., Saunders, C., Latham, J., Christian, H., 2001. Modeling and observations of thundercloud electrification and lightning. Atmos. Res. 58, 89-115.

Mitzeva, R., Saunders, C. P. R., 1990. Thunderstorm charging-calculations of the effect of ice crystal size and graupel velocity. J. Atmos. Sol. Terr. Phys. 52, 241-245.

Mohr, K. I., Toracinta, E. R., Ziper, E. J., Orville, R. E., 1996. A comparison SSMI brightness temperatures, and lightning for Mesoscale Convective Systems in Texas part brightness temperatures and lightning. J. Appl. Meteorol. 35, 919-931.

Mohr, K. I., Ziper, E. J., 1996. Defining Mesoscale Convective System by their 85-GHz ice-scattering signatures. Bull. Am. Meteorol. Soc. 77, 1179-1189.

Orville, R. E., Huffines, G., Gammon, J. N., Zhang, R., Ely, B., Steige, S., Phillips, S., Allen, S., Read, W., 2000. Enhancement of Cloud-to-Ground Lightning over Houston, Texas. Geophys. Res. Lett. 28 (13), 2597-2600.

Parker, M. D., Rutledge, S. B., Johnson, R. H., 2001. Cloud-to-Ground lightning in Linear Mesoscale Convective Systems. Mon. Weather Rev. 129, 1232-1242.

Petersen, W. A., Christian, H. J., Rutledge, S. A., 2005. TRMM observations of the global relationship between ice water content and lightning. Geophys. Res. Lett. 32, L14819, doi:10.1029/2005GL023236.

Pinto Jr, O., Pinto, I. R. C. B., Diniz, J. H., Cazetta Filho, B., Cherchiglia, L. C. L., Carvalho, B. M., 2003. A seven-year study about the negative cloud-to-ground lightning flash characteristics in Southeastern Brazil. J. Atmos. Sol. Terr. Phys. 65, 739-748.

Pinto Jr., O., Pinto, I. R. C. A., Naccarato, K.P., 2007. Maximum cloud-to-ground lightning flash densities observed by lightning location systems in the tropical region: a review. Atmos. Res. 84, 189–200.

Prigent, C., Defer, E., Pardo, J. R., Pearl, C., Rossow, W. B., Pinty, J. P., 2005. Relations of polarized scattering signatures observed by the TRMM Microwave instrument with electrical processes in cloud systems. Geophys. Res. Lett. 32, L04810,doi:10.1029/2004GL022225.

Prigent, C., Pardo, J. R., Mishchenko, M. I., Rossow, W. B., 2001. Microwave polarized signatures generated within cloud systems: Special Sensor Microwave Imager (SSM/I) observations interpreted with radiative transfer simulations. J. Geophys. Res. Atmos. 106, 28,243–28,258, doi:10.1029/2001JD900242.

Reynolds S. E., Brook M., Gourley M. F., 1957. Thunderstorm charge separation. J. Meteorol. 14, 426-436 .

Saunders, C. P. R. A., 1993. Review of thunderstorm electrification processes. J. Appl. Meteorol. 32, 642- 655.

Saunders, C. P. R., Keith, W. D., Mitzeva, R. P., 1991. The effect of liquid water on thunderstorm charging. J. Geophys. Res. Atmos. 96, 11007-11017.

Schulz, W., Cummins, K., Diendorfer, G., Dorninger, M., 2005. Cloud-to-Ground lightning in Austria: a 10-year study using data from a lightning location system. J. Geophys. Res. Atmos. 110, D09101.doi:10.1029/2004JD005332.

Scofield, R. B., Kuligowski, R. J., Qiu, S., 2005. Combining lightning with satellite data for analysis and prediction. Proceedings of Conference on Meteorological Applications of Lightning Data. American Meteorological Society, San Diego, California.

Spencer, R. W., Goodman, H. M., Hood, R. E., 1989. Precipitation retrieval over land and ocean with the SSM/I: identification and characteristics of the scattering signal. J. Atmos. Oceanic Technol. 6, 254-273.

Stubenrauch, C. J., Eddounia, F., Rädel, G., 2004. Correlations between microphysical properties of large-scale semi-transparent cirrus and the state of the atmosphere. Atmos. Res. 72, 403-423. doi:10.1016/j.atmosres.2004.03.024.

Tadesse, B., Anagnostou, E. N., 2009. Characterization of warm season convective systems over US in terms of cloud to ground lightning, cloud kinematics ,and precipitation. Atmos. Res. 91, 36-46.

Tsenova, B., Mitzeva, R., Saunders, C., 2009. A modeling study of the effect of ice particle sizes and relative velocity on ice crystal/graupel collisional charge transfer. Atmos. Res. 91, 250-258.

Ushio, T., Heckman, S. J., Boccippio, D. J., Christian, H. J., 2001. A Survey of thunderstorm flash rates compared to cloud top height using TRMM satellite data. J. Geophys. Res. Atmos. 106, 89-95.

Velasco, I., Fritsch, J., 1987. Mesoscale Convective Complexes in the Americas. J. Geophys. Res. Atmos. 92 (D8), 9591-9613.

Vila, D. B., Machado, L. B. T., Laurent, H., Velasco, I., 2008. Forecast and tracking the evolution of cloud clusters (ForTracCC) using satellite infrared imagery: methodology and validation. Weather Forecasting. 23, 233-245

Vonnegut, B., 1963. Some facts and speculations concerning the origin and role of thunderstorm electricity, Meteorology Monograph, 5, 224-241.

Wallace, M. J., Hobbs, V. P., 1977. Atmospheric science: an introductory survey. First ed. Academic Press, Washington.

Weng, F., 1992. A multi-layer discrete-ordinate method for vector radiative transfer in a vertically-inhomogeneous, emitting and scattering atmosphere. Part I: Theory J. Quant. Spec. Radiat.Trans. 47, 19–33.

Weng, F., Grody, N. C., 2000. Retrieval of ice cloud parameters using a microwave imaging radiometer. J. Atmos. Sci. 57, 1069–1081.

Williams, E. R., 1985. Large-scale charge separation in thunderclouds, J. Geophys. Res. 90, 6013-6025.

Zhao, L., Weng, F., 2001. Retrieval of ice cloud parameters using the advanced microwave sounding unit. J. Appl. Meteorol. 41, 384-395.

TABLE CAPTIONS

Table 1- Coefficients used to determine D_e and IWP.
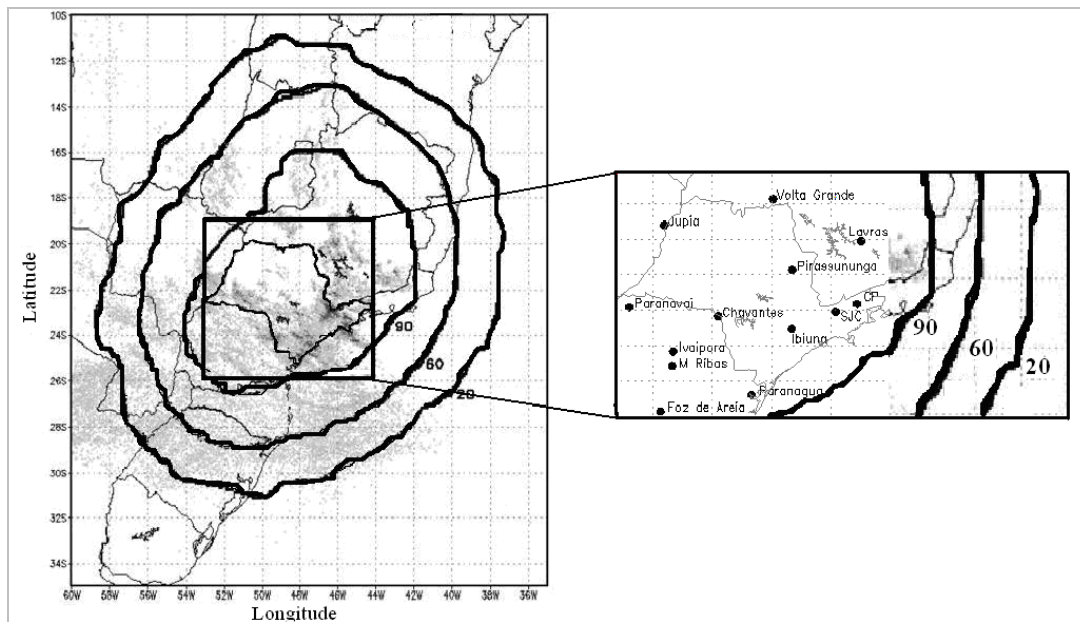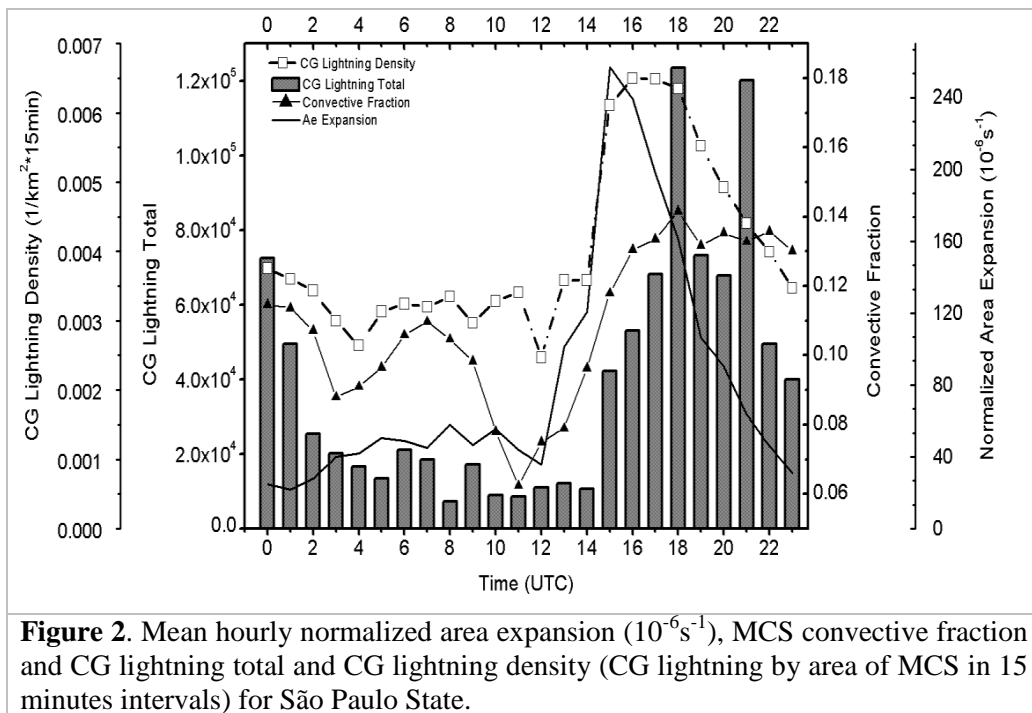
FIGURE CAPTIONS

Figure 1. Region of study, location of BrasilDAT sensors inside this region and contour lines of CG lightning detection efficiency within 20, 60 and 90 %.
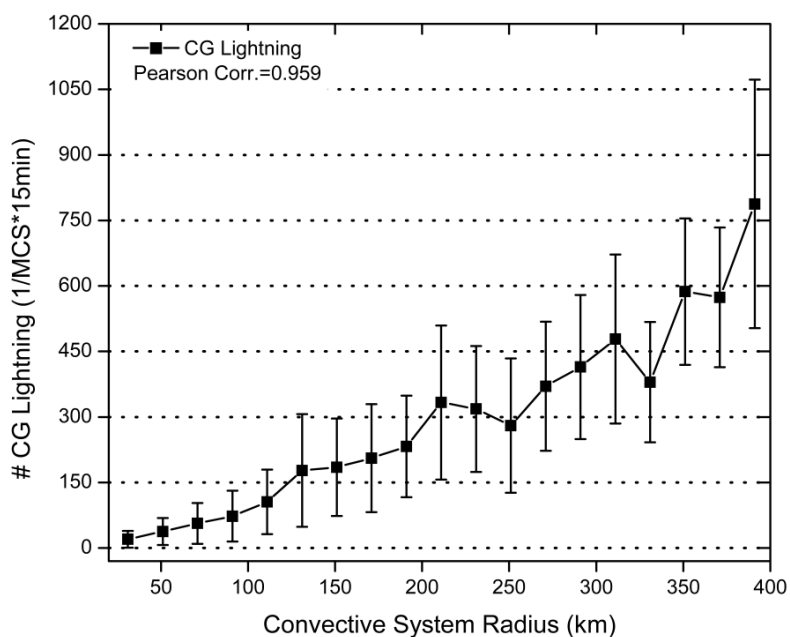
Figure 2. Mean hourly normalized area expansion ($10^{-6}s^{-1}$), MCS convective fraction and CG lightning total and CG lightning density (CG lightning by area of MCS in 15 minutes intervals) for São Paulo State.

Figure 3. Variation of average and standard deviation of MCS CG lightning occurrence in 15 minute intervals (# CG lightning/15min) as a function of the effective radius (km) of the convective system.

Figure 4. Variation of average and standard deviation of MCS CG lightning occurrence in 15 minute intervals (# CG lightning/15min) as a function of the IR Minimum Temperature (K) of the convective system.
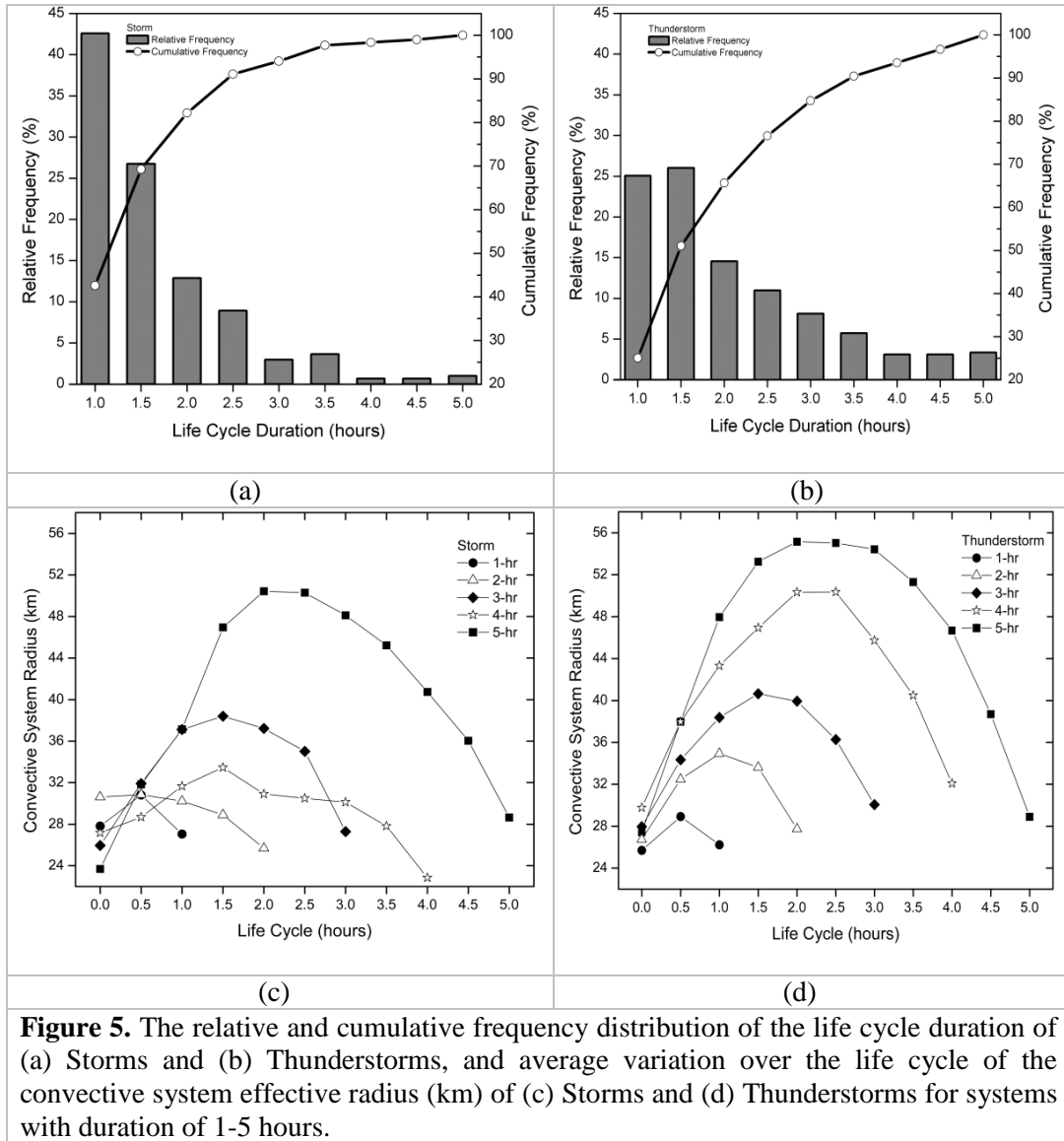
Figure 5. The relative and cumulative frequency distribution of the life cycle duration of (a) Storms and (b) Thunderstorms, and average variation over the life cycle of the convective system effective radius (km) of (c) Storms and (d) Thunderstorms for systems with duration of 1-5 hours.
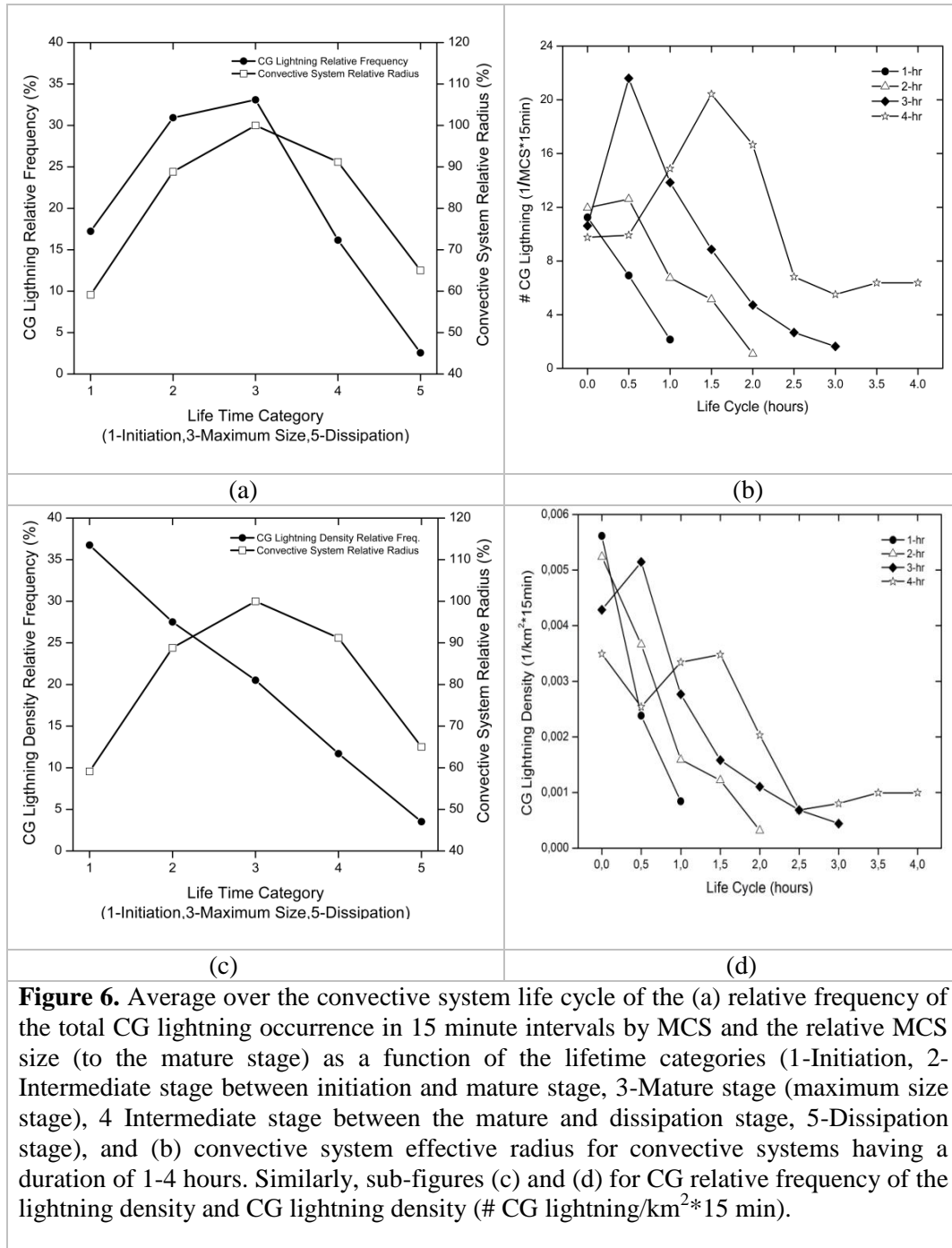
Figure 6. Average over the convective system life cycle of the (a) relative frequency of the total CG lightning occurrence in 15 minute intervals by MCS and the relative MCS size (to the mature stage) as a function of the lifetime categories (1-Initiation, 2-Intermediate stage between initiation and mature stage, 3-Mature stage (maximum size stage), 4 Intermediate stage between the mature and dissipation stage, 5-Dissipation stage), and (b) convective system effective radius for convective systems having a duration of 1-4 hours. Similarly, sub-figures (c) and (d) for CG relative frequency of the lightning density and CG lightning density (# CG lightning/km^2*15 min).
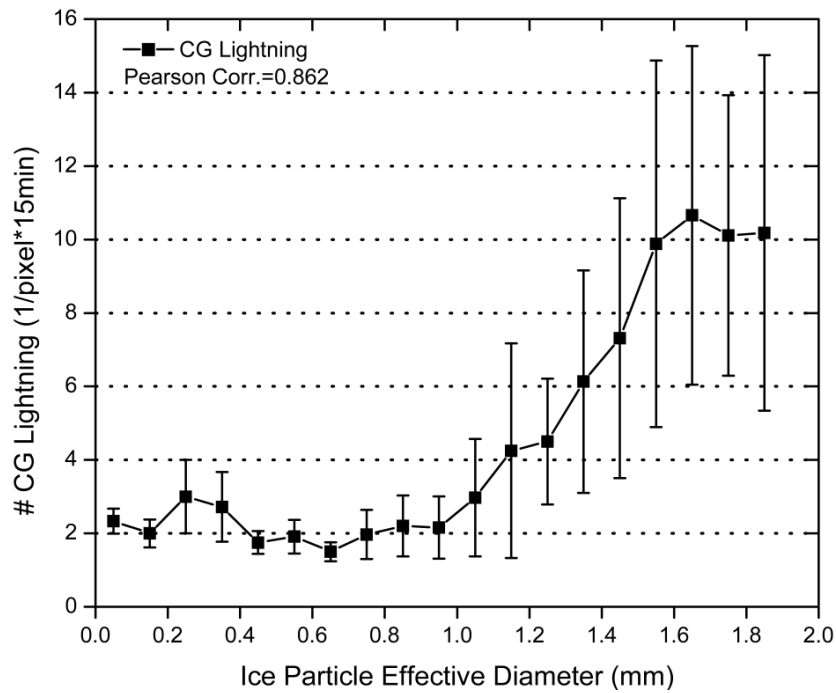
Figure 7. Variation of average and standard deviation of CG lightning occurrence in 15 minute intervals by pixel (# CG lightning/pixel*15min) as a function of Ice Particle Effective Diameter (mm).
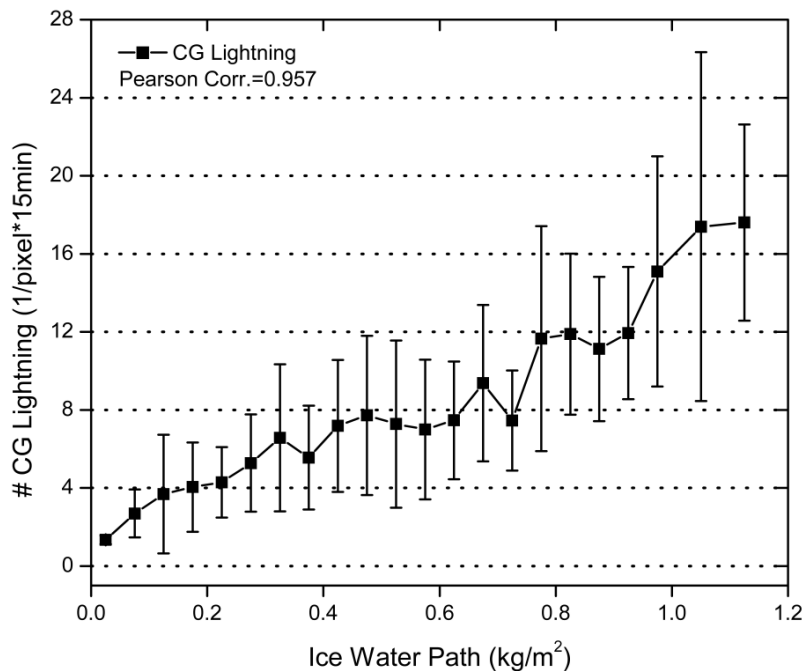
Figure 8. Variation of average and standard deviation of CG lightning occurrence in 15 minute intervals by pixel (# CG lightning/pixel*15min) as a function of Ice Water Path (kg/m^2).
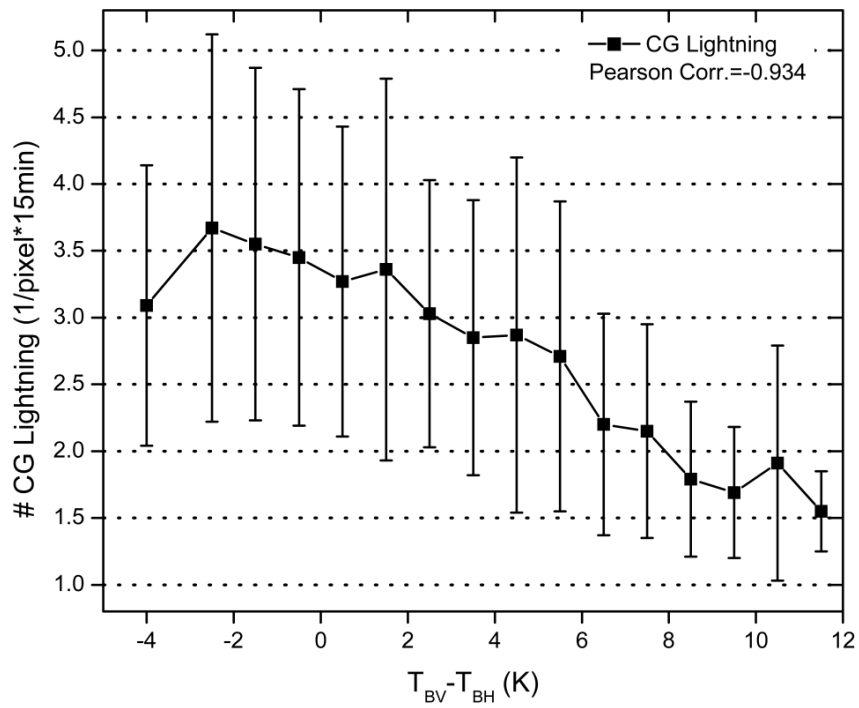
Figure 9. Variation of average and standard deviation of CG lightning occurrence in 15 minute intervals by pixel (# CG lightning/pixel*15min) as a function of the Polarized Temperature Difference at 85 GHz ($T_{BV}-T_{BH}$).

Table 1- Coefficients used to determine D_e and IWP.

		a_0	a_1	a_2	a_3
De		-0.3003	4.3088	-3.9826	2.7832
		b_0	b_1	b_2	
IWP	$D_e \geq 1.0$ mm	-1.1930	2.0883	-0.8575	
	$D_e < 1.0$ mm	-0.2945	1.3884	-0.7536	

Figure 1. Region of study, location of BrasilDAT sensors inside this region and contour lines of CG lightning detection efficiency within 20, 60 and 90 %.

Figure 2. Mean hourly normalized area expansion ($10^{-6}s^{-1}$), MCS convective fraction and CG lightning total and CG lightning density (CG lightning by area of MCS in 15 minutes intervals) for São Paulo State.

Figure 3. Variation of average and standard deviation of MCS CG lightning occurrence in 15 minute intervals (# CG lightning/15min) as a function of the effective radius (km) of the convective system.

Figure 4. Variation of average and standard deviation of MCS CG lightning occurrence in 15 minute intervals (# CG lightning/15min) as a function of the IR Minimum Temperature (K) of the convective system.

.

Figure 5. The relative and cumulative frequency distribution of the life cycle duration of (a) Storms and (b) Thunderstorms, and average variation over the life cycle of the convective system effective radius (km) of (c) Storms and (d) Thunderstorms for systems with duration of 1-5 hours.

(a)

(b)

(c)

(d)

Figure 6. Average over the convective system life cycle of the (a) relative frequency of the total CG lightning occurrence in 15 minute intervals by MCS and the relative MCS size (to the mature stage) as a function of the lifetime categories (1-Initiation, 2-Intermediate stage between initiation and mature stage, 3-Mature stage (maximum size stage), 4 Intermediate stage between the mature and dissipation stage, 5-Dissipation stage), and (b) convective system effective radius for convective systems having a duration of 1-4 hours. Similarly, sub-figures (c) and (d) for CG relative frequency of the lightning density and CG lightning density (# CG lightning/km^2*15 min).

Figure 7. Variation of average and standard deviation of CG lightning occurrence in 15 minute intervals by pixel (# CG lightning/pixel*15min) as a function of Ice Particle Effective Diameter (mm).

Figure 8. Variation of average and standard deviation of CG lightning occurrence in 15 minute intervals by pixel (# CG lightning/pixel*15min) as a function of Ice Water Path (kg/m^2).

Figure 9. Variation of average and standard deviation of CG lightning occurrence in 15 minute intervals by pixel (# CG lightning/pixel*15min) as a function of the Polarized Temperature Difference at 85 GHz (T_{BV}-T_{BH}).

Figure1
Click here to download high resolution image
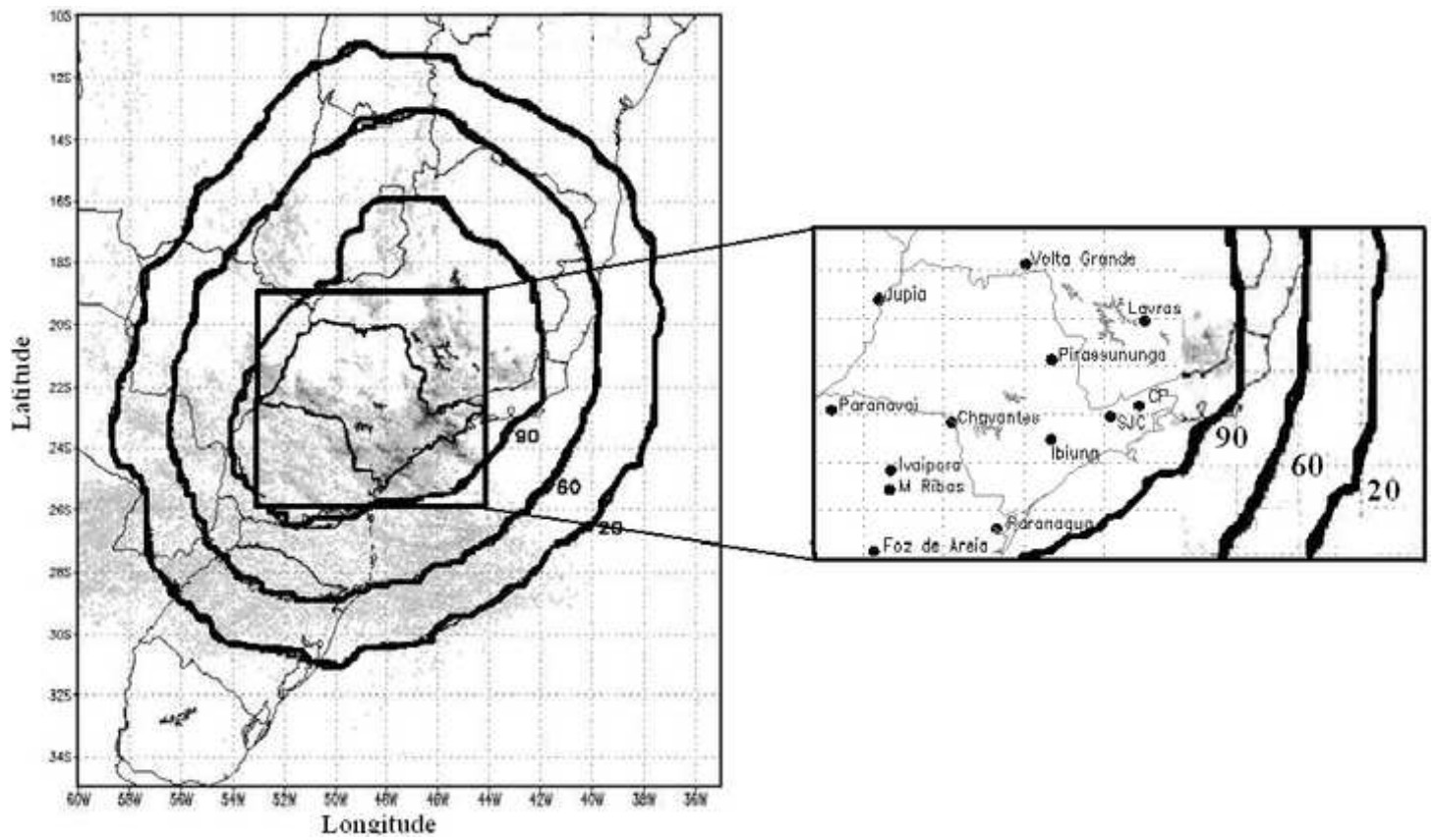
Figure2
Click here to download high resolution image
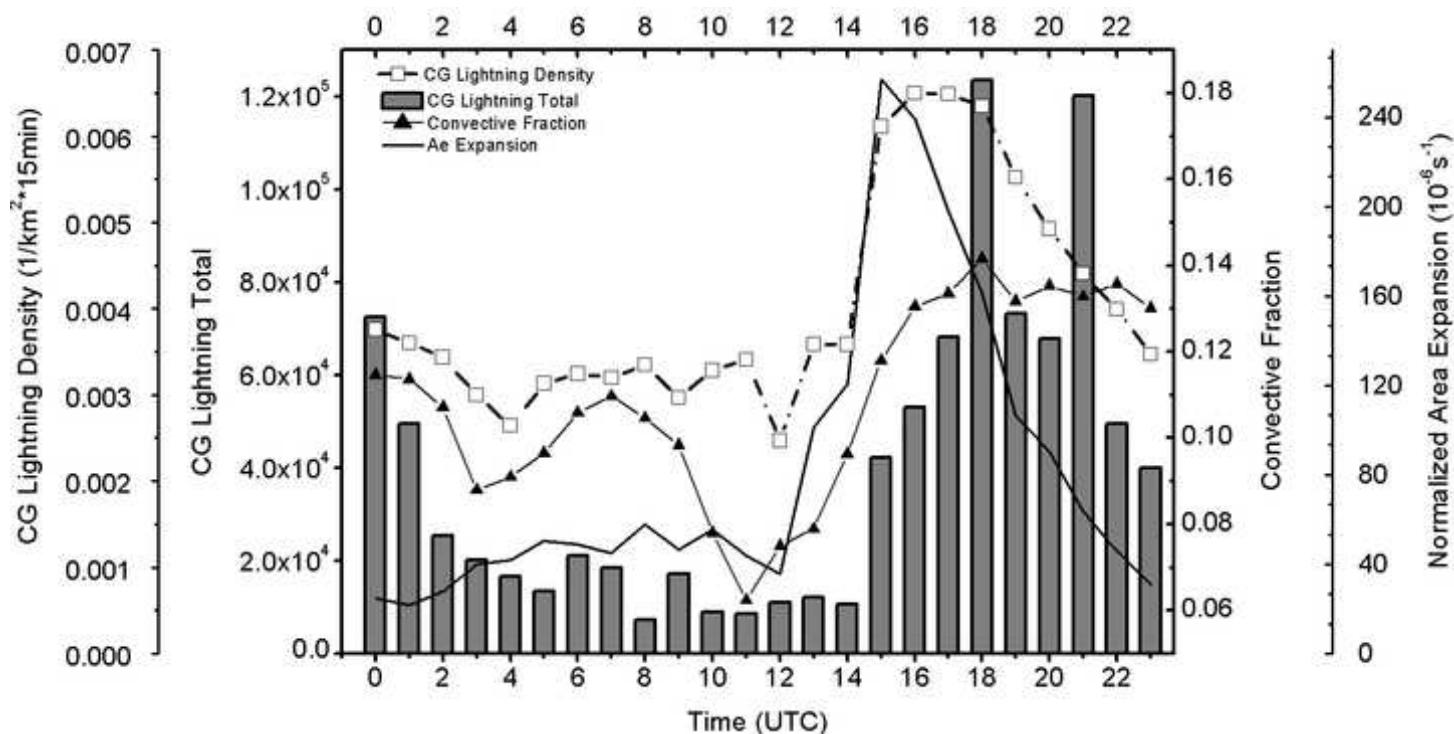
Figure3
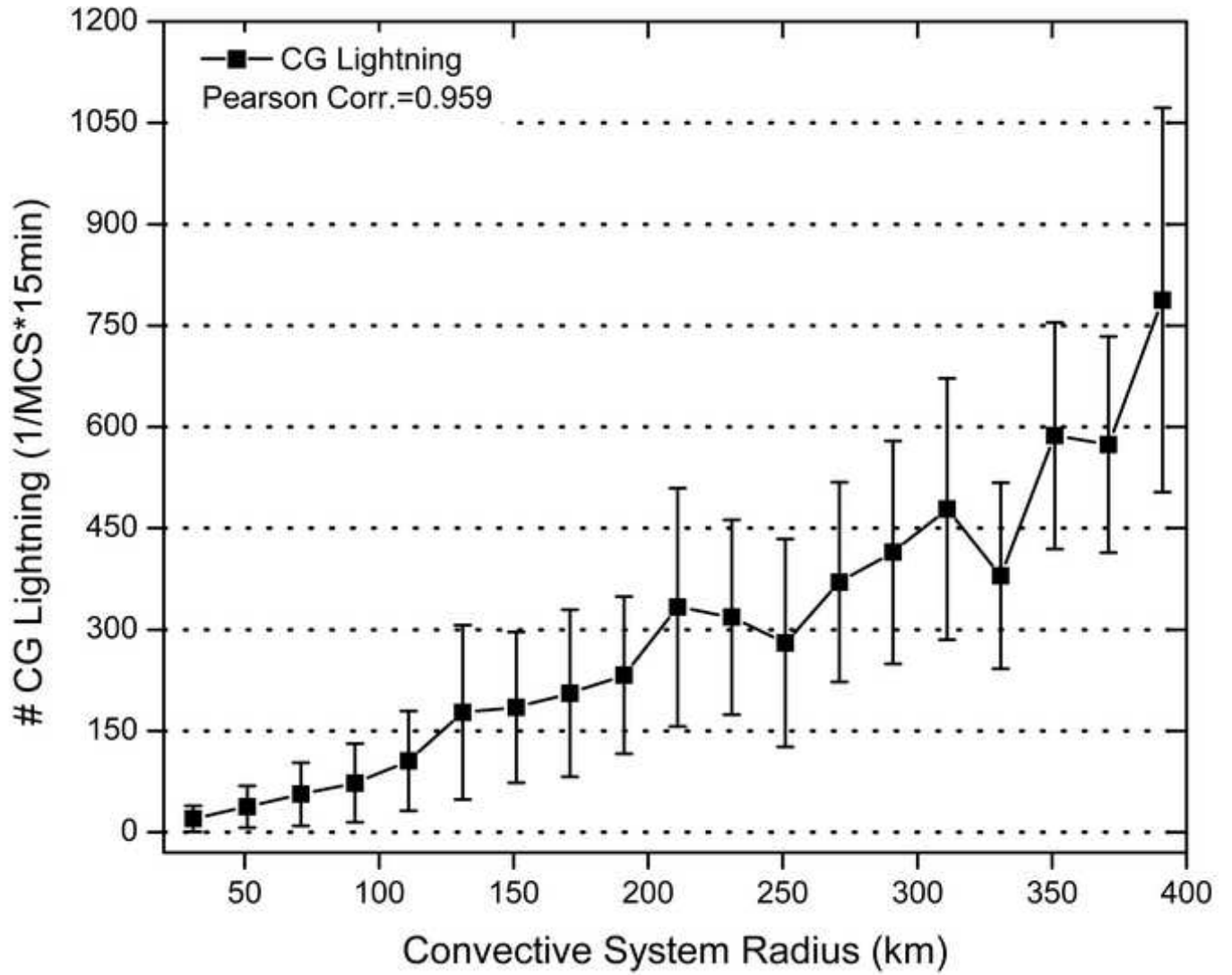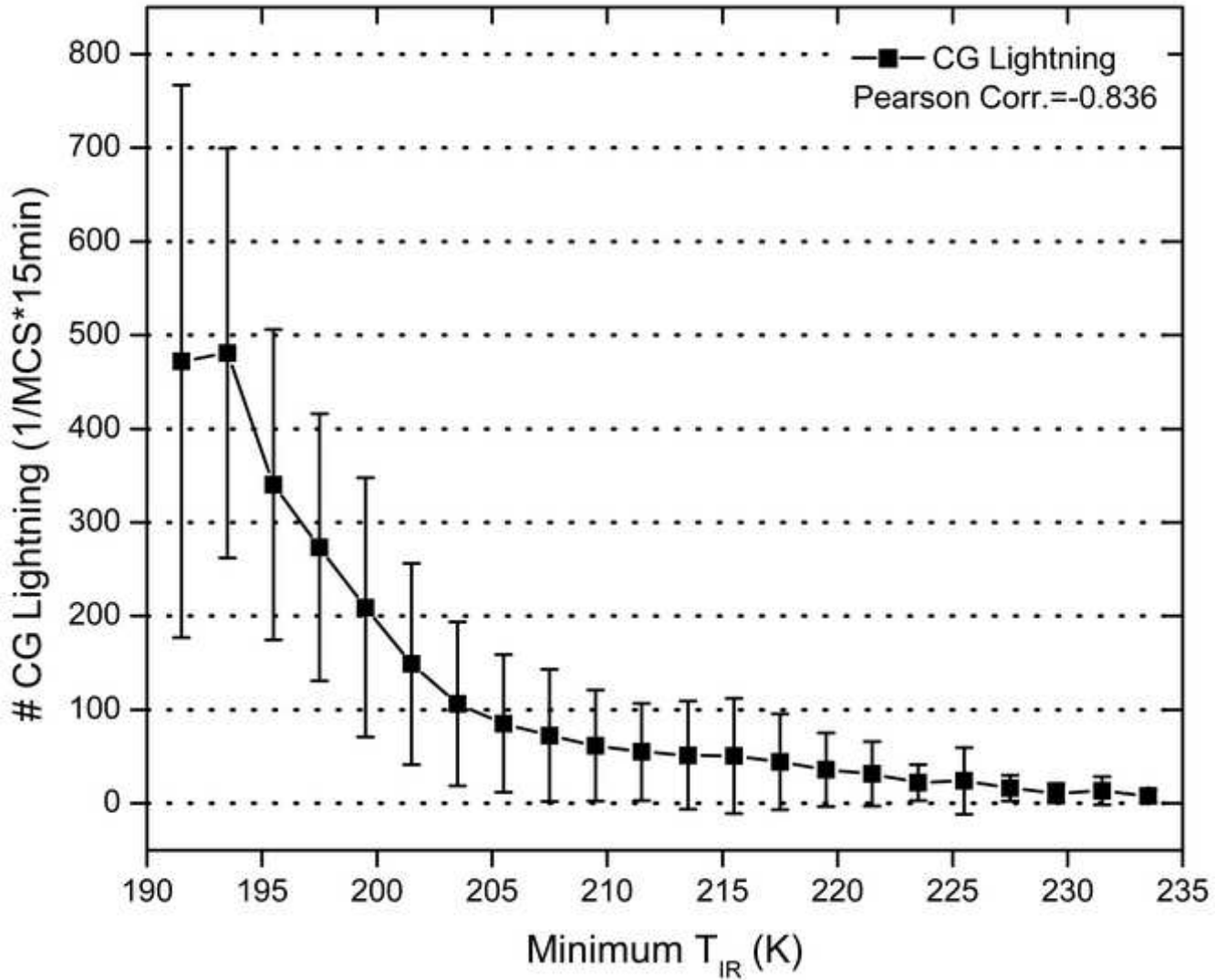
Figure4

Figure5a
Click here to download high resolution image
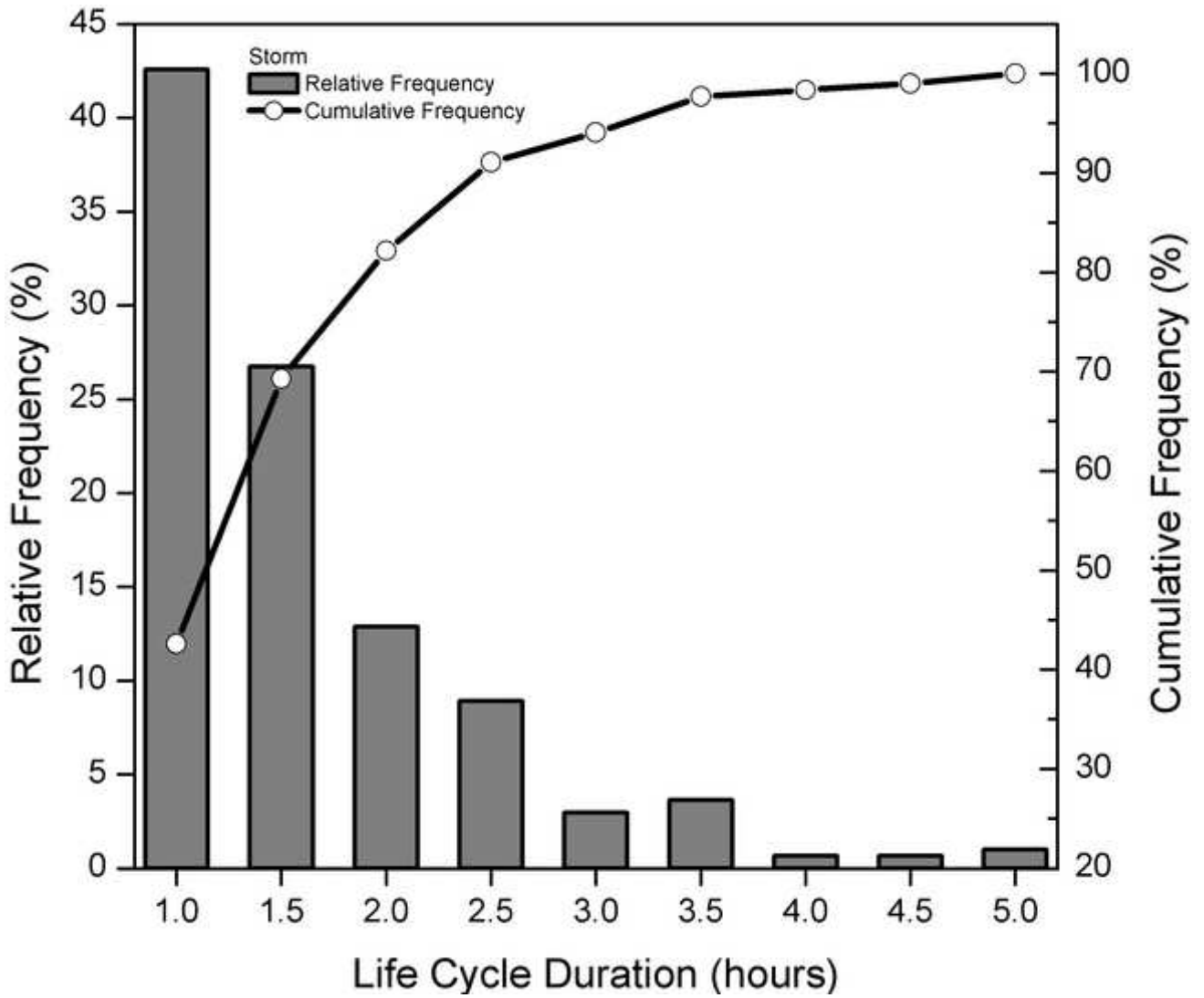
Figure5b
Click here to download high resolution image
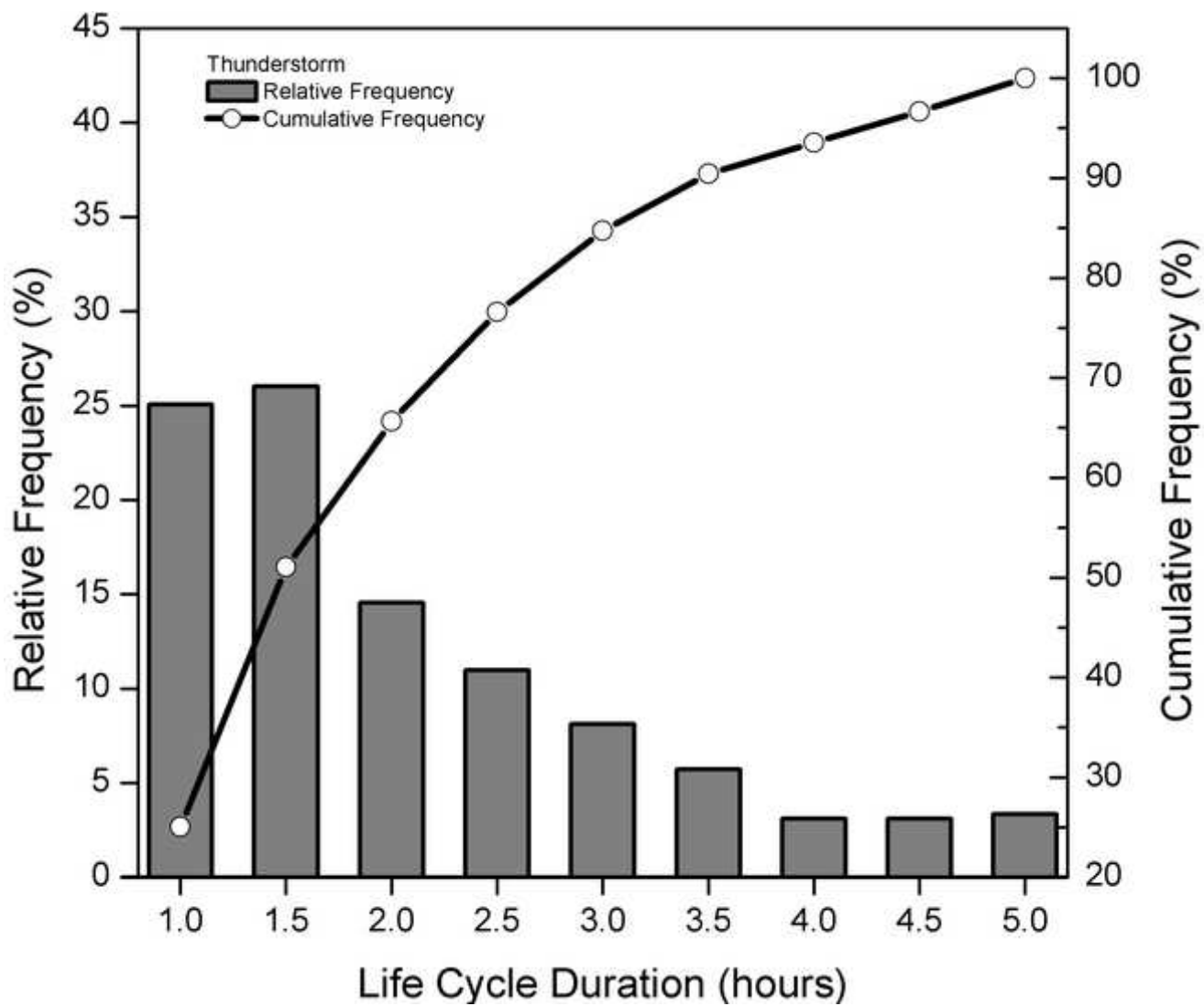
Figure5c
Click here to download high resolution image
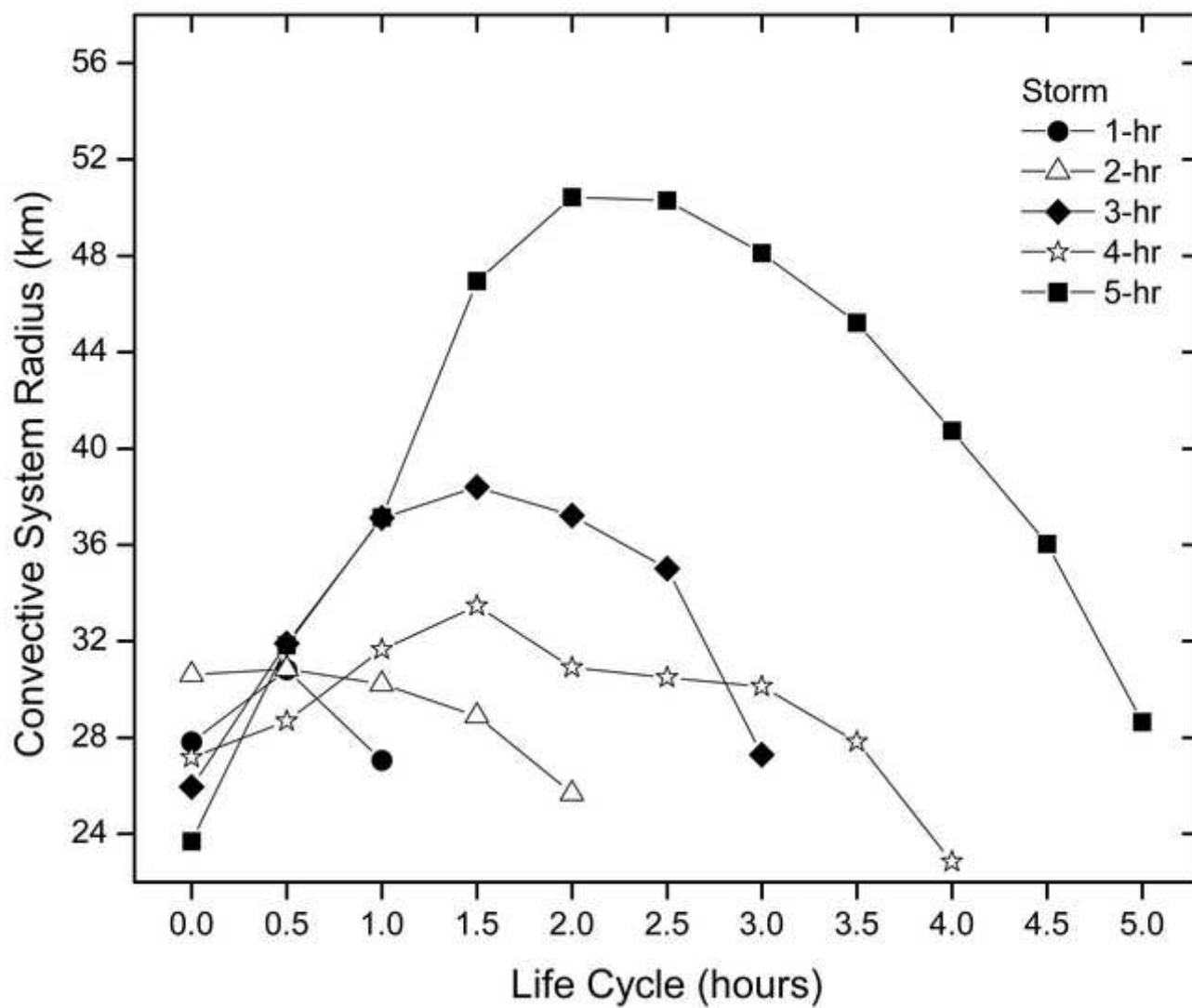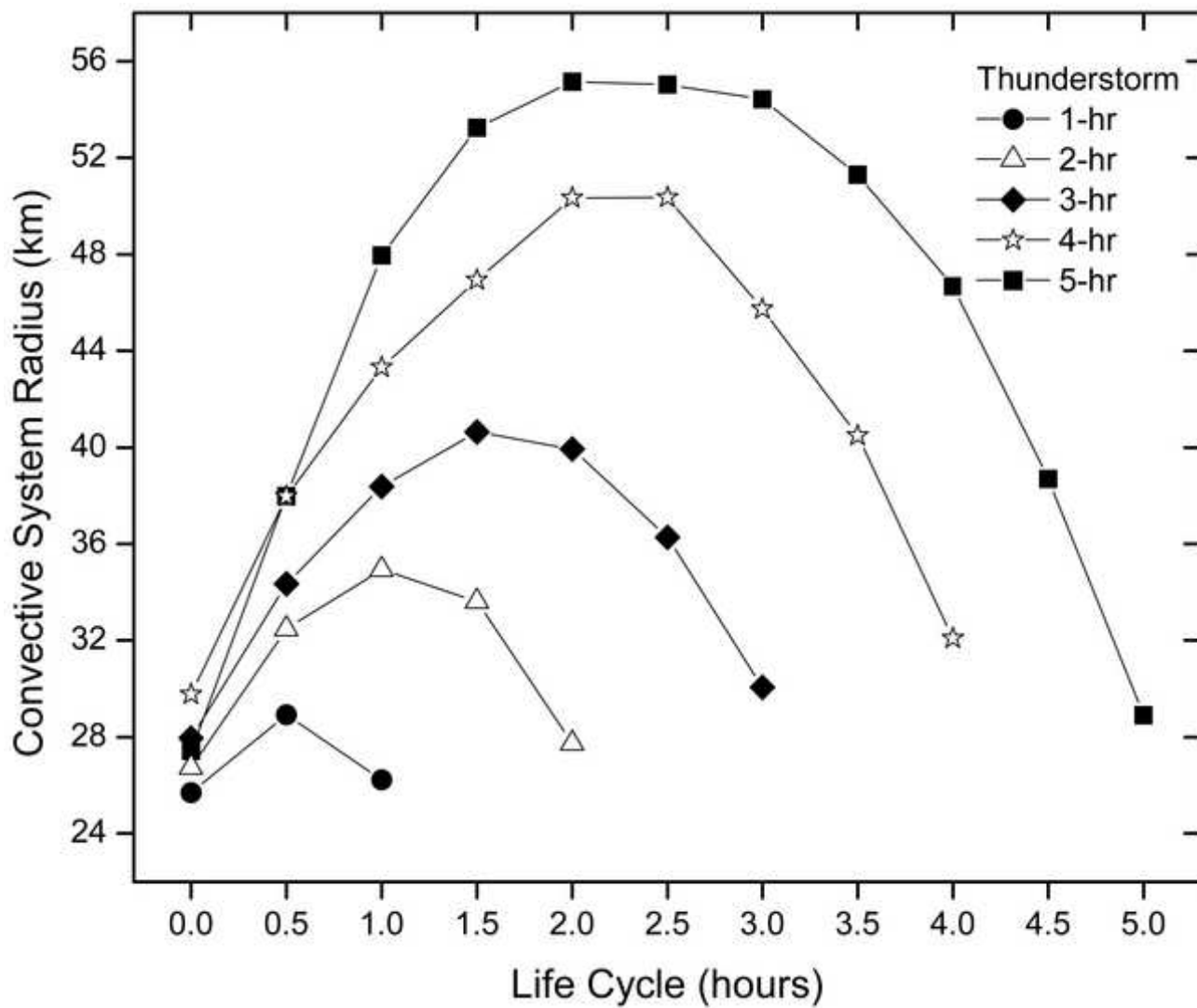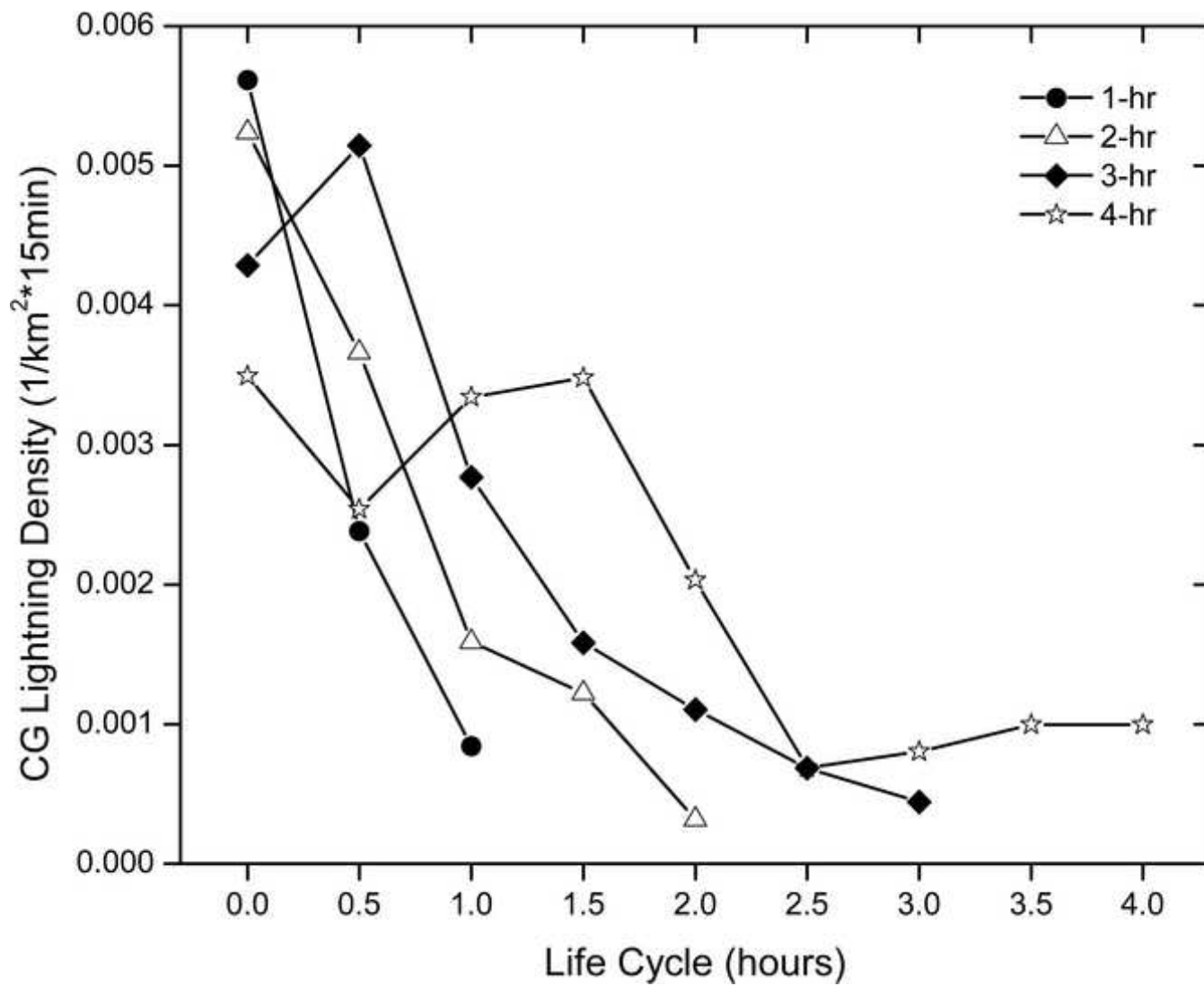
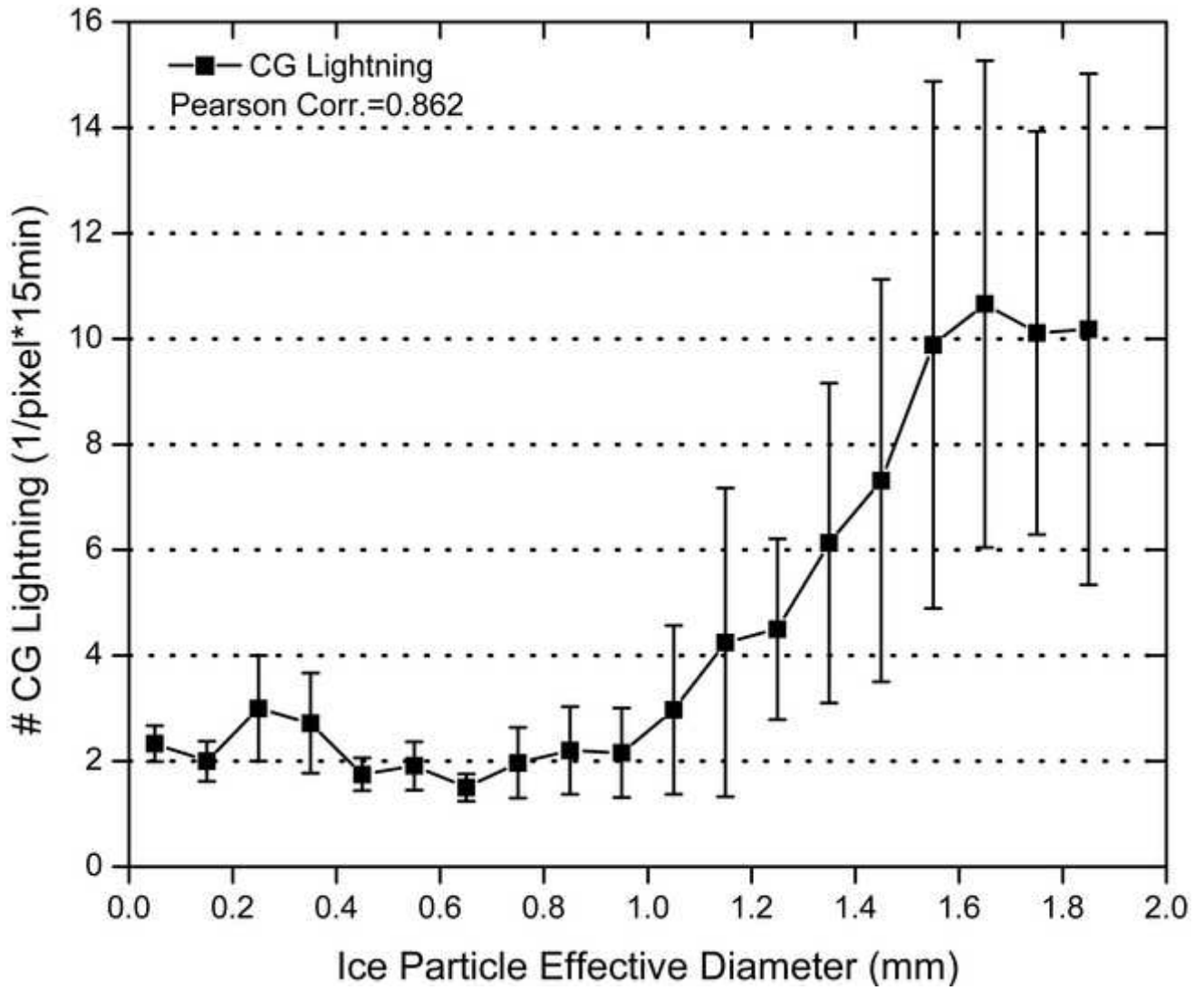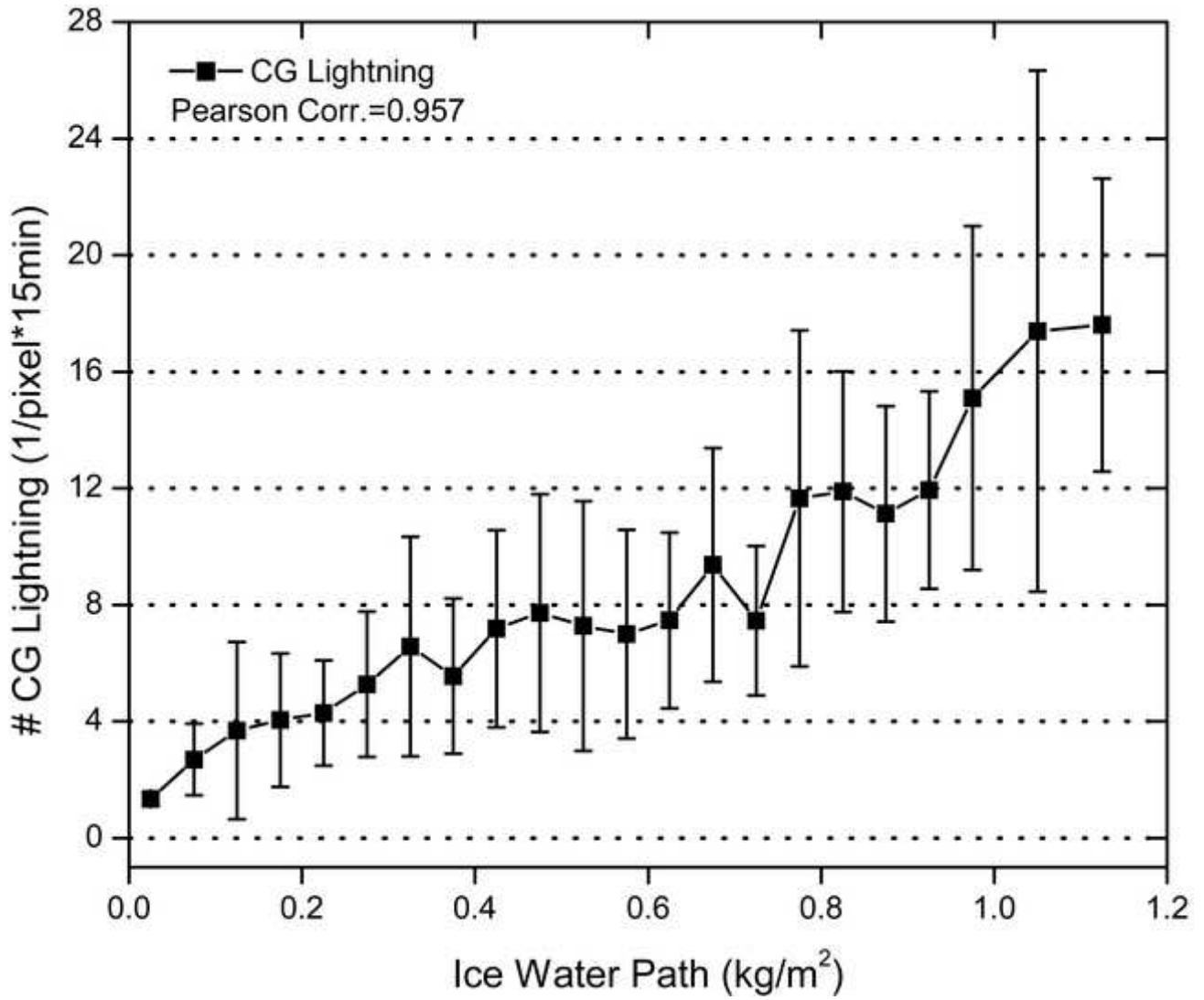**Figure6a**
Click here to download high resolution image
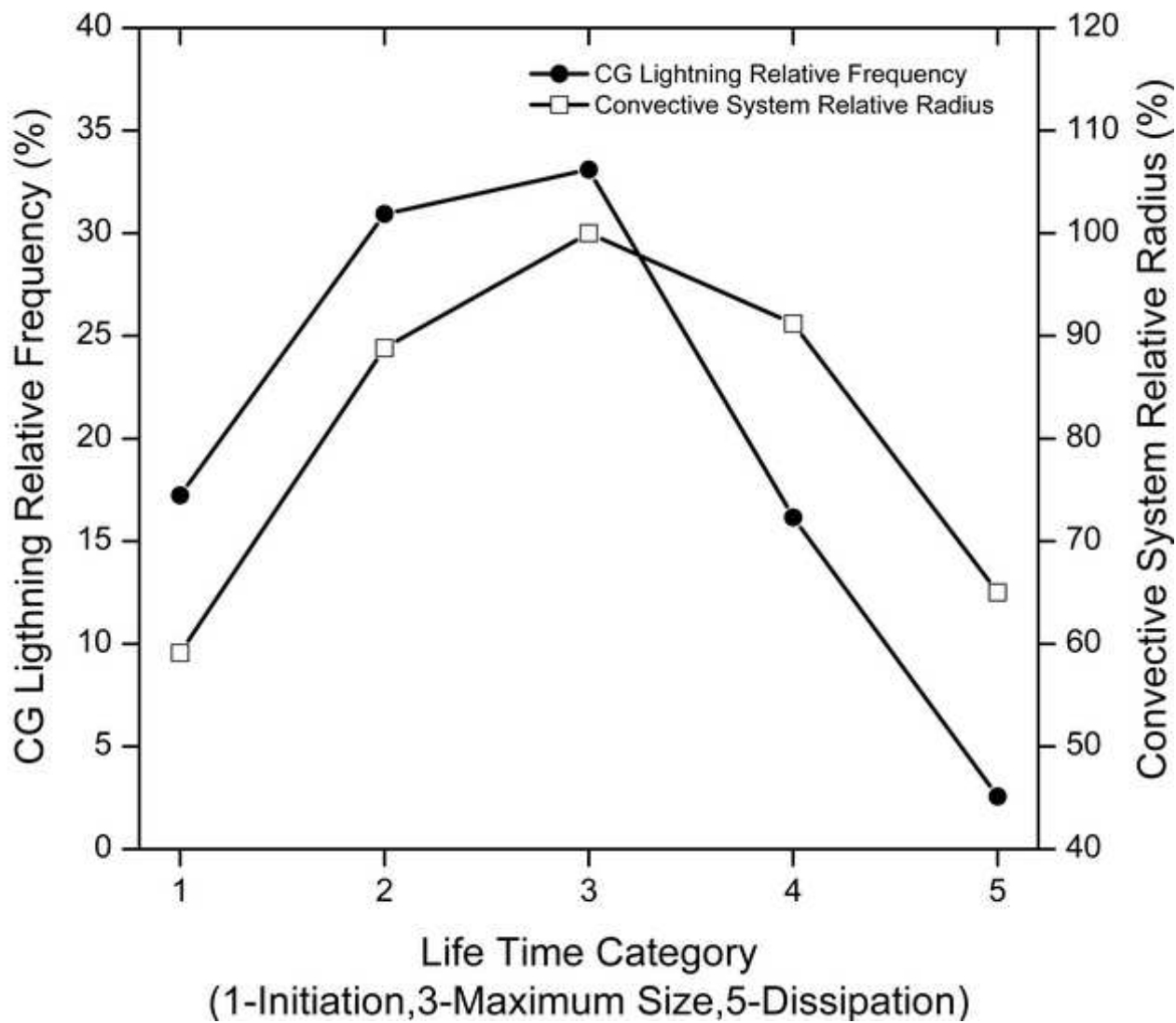
Figure6b
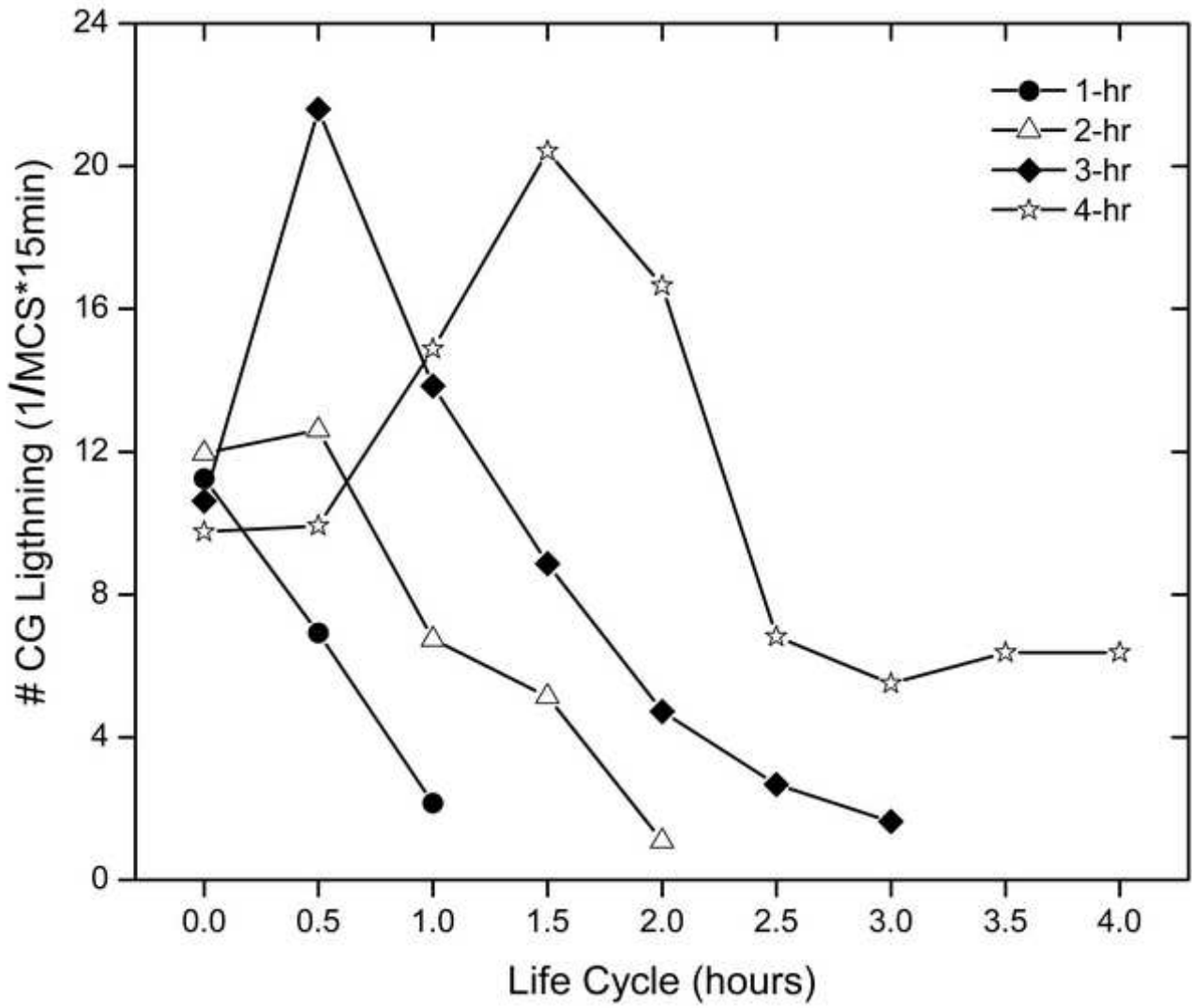
Figure6c
Click here to download high resolution image
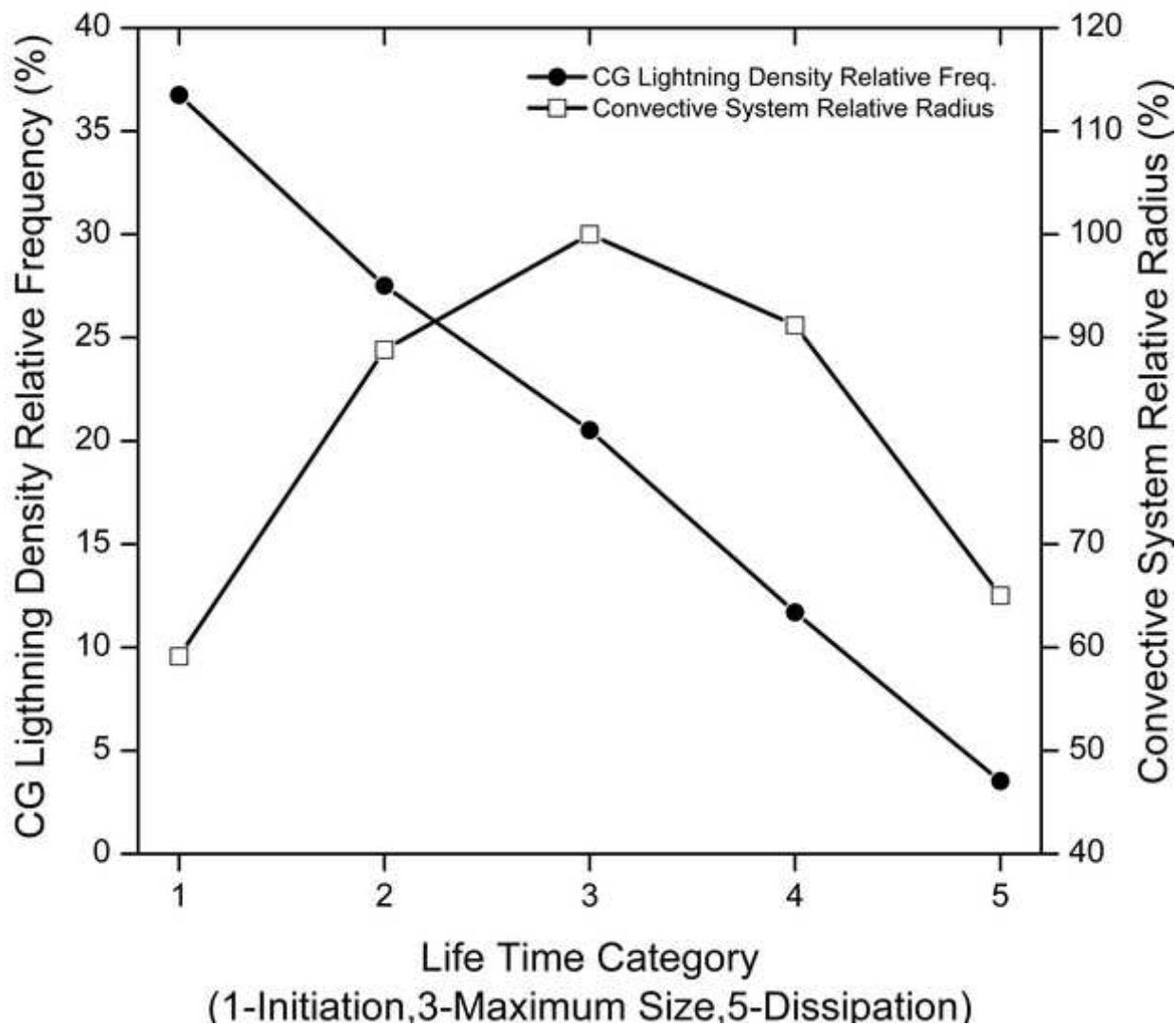
Figure6d

Figure7
Click here to download high resolution image

Figure8
Click here to download high resolution image

Figure9

Table

	a_0	a_1	a_2	a_3
De	-0.3003	4.3088	-3.9826	2.7832
		b_0	b_1	b_2
IWP $D_e \geq 1.0$ mm		-1.1930	2.0883	-0.8575
$D_e < 1.0$ mm		-0.2945	1.3884	-0.7536